Remote Sensing Applications: Society and Environment 36 (2024) 101345

Contents lists available at ScienceDirect

Remote Sensing Applications: Society and Environment

journal homepage: www.elsevier.com/locate/rsase

Mangrove forest regeneration age map and drivers of restoration success in Gulf Cooperation Council countries from satellite imagery

Midhun Mohan [a, b, c, d, e, f, *], Abhilash Dutta Roy [a, f, g, h], Jorge F. Montenegro [a, c, d, f, i], Michael S. Watt [j], John A. Burt [k], Aurelie Shapiro [l], Dhouha Ouerfelli [a, m], Redeat Daniel [a, n], Sergio de-Miguel [o, p], Tarig Ali [c], Macarena Ortega Pardo [q], Mario Al Sayah [r], Valliyil Mohammed Aboobacker [s], Naji El Beyrouthy [x], Ruth Reef [t], Esmaeel Adrah [u], Reem AlMealla [v], Pavithra S. Pitumpe Arachchige [a, f], Pandi Selvam [w], Wan Shafrina Wan Mohd Jaafar [e], Lara Sujud [x], Jenan Bahzad [y], Isuru Alawatte [z], Sohaib Hussein [aa], Carlos López-Martínez [ab], Frida Sidik [ac], Manickam Nithyanandan [ad], Meshal Abdullah [ae, af], Mohammad Al-Khalid [ag], Ammar Abulibdeh [d], Adrián Cardil [o, p, ah], Jeffrey Q. Chambers [b, ai]

[a] *Ecoresolve, San Francisco, CA, United States*
[b] *Department of Geography, University of California - Berkeley, Berkeley, CA, United States*
[c] *Department of Civil Engineering, College of Engineering, American University of Sharjah (AUS), PO Box 26666, Sharjah, United Arab Emirates*
[d] *Applied Geography and GIS Program, Department of Humanities, College of Arts and Sciences, Qatar University, Doha, Qatar*
[e] *Earth Observation Centre, Institute of Climate Change, Universiti Kebangsaan Malaysia, 43600 Selangor, Malaysia*
[f] *Morobe Development Foundation (via United Nations Volunteering Program), Lae, Papua New Guinea*
[g] *Mediterranean Forestry and Natural Resources Management, School of Agriculture, University of Lisbon, Lisbon, Portugal*
[h] *School of Agrifood and Forestry Engineering and Veterinary Medicine, University of Lleida, Lleida, Spain*
[i] *University of Liverpool Management School, University of Liverpool, Liverpool, United Kingdom*
[j] *Scion, 10 Kyle St, Christchurch 8011, New Zealand*
[k] *Center for Interacting Urban Networks (CITIES) and Mubadala Arabian Center for Climate and Environmental Sciences (Mubadala ACCESS), New York University Abu Dhabi, PO Box 129188, Abu Dhabi, United Arab Emirates*
[l] *Here+There Mapping Solutions, Berlin, Germany*
[m] *Mediterranean Agronomic Institute of Chania, Greece*
[n] *Adama Science and Technology University, Adama, Oromia, Ethiopia*
[o] *Department of Agricultural and Forest Sciences and Engineering, University of Lleida, Lleida, Spain*
[p] *Forest Science and Technology Centre of Catalonia (CTFC), Solsona, Spain*
[q] *Forest Fire Laboratory, Department of Forest Engineering, University of Córdoba, 14071, Córdoba, Spain*
[r] *National Council for Scientific Research, Remote Sensing Center, Lebanon*
[s] *Environmental Science Center, Qatar University, Doha, Qatar*
[t] *School of Earth Atmosphere and Environment, Monash University, Melbourne, Australia*
[u] *Kent State University, Kent, OH, United States*
[v] *Nuwat for Environmental Research & Education, Al Janabiyah, Bahrain*
[w] *GAIT Global, Singapore*
[x] *Department of Agriculture, Faculty of Agricultural and Food Sciences, American University of Beirut, Beirut, Lebanon*

* Corresponding author. Ecoresolve, San Francisco, CA, United States.
E-mail address: mikey@ecoresolve.eco (M. Mohan).

https://doi.org/10.1016/j.rsase.2024.101345
Received 21 May 2024; Received in revised form 7 July 2024; Accepted 6 September 2024
Available online 12 September 2024

[y] Public Authority of Applied Education and Training, Kuwait
[z] Deputy Conservator of Forests, Department of Forest Conservation, Sri Lanka
[aa] BLUE FOREST, Dubai, United Arab Emirates
[ab] Department of Signal Theory and Communications, Universitat Politècnica de Catalunya, Barcelona, Spain
[ac] Research Centre for Oceanography, National Research and Innovation Agency, Jakarta, Indonesia
[ad] Environment and Life Sciences Research Center, Kuwait Institute for Scientific Research, Kuwait
[ae] Department of Geography, College of Arts and Social Sciences, Sultan Qaboos University, Muscat, Oman
[af] Department of Ecology and Conservation Biology, Texas A&M University, College Station, TX, United States
[ag] Netzero, Saudi Arabia
[ah] Tecnosylva, León, Spain
[ai] Lawrence Berkeley National Laboratory, Berkeley, CA, 94720, United States

ARTICLE INFO

Keywords:
Mangrove remote sensing
Google earth engine
Landsat imagery
Middle east forests
Ecosystem conservation
Secondary forest map
Logistic regression analysis

ABSTRACT

Mangrove forests are found across the Gulf Cooperation Council (GCC) region despite challenging environmental extremes, including highly variable temperatures and hypersalinity. Understanding the biophysical and anthropogenic factors that influence mangrove forest growth is key to locate suitable areas for regeneration and afforestation activities. The main objectives of this study were to develop a mangrove forest regeneration age map that represents the age of all the existing secondary mangroves in the past 37 years (1986–2023). Long-term Landsat satellite imagery, the random forest classification algorithm, and logistic regression analyses were used to identify the existing secondary mangroves and determine the underlying drivers that contribute to the successful afforestation of mangroves in the region. Our results showed that only around 8.5% of secondary mangrove forests in the GCC region were older than 30 years, with mangroves younger than 5 years being the most abundant age class (41.3%). Saudi Arabia and Oman have the highest percentages of young mangroves, while relatively older secondary mangrove forests were most common in Bahrain, Qatar, and UAE. The current trends in overall mangrove area show that the UAE and Saudi Arabia have the largest total mangrove area among the GCC countries, followed by Qatar, Oman, Bahrain, and Kuwait. The results of the stepwise logistic regression show that the main drivers that influence mangrove regeneration are lower elevation, lower slope, higher available soil moisture, lower average temperatures, higher precipitation, greater proximity to freshwater sources, lower population density and greater distance from agricultural and urban areas. Our results aim to offer support to decision-making in selecting optimal areas for new planting initiatives in the region.

1. Introduction

Mangrove ecosystems consist of multiple tree and shrub species located in intermittently inundated intertidal zones (Assaf et al., 2022). They are considered ecologically and economically important in all coastal regions across the tropics (Leandro et al., 2022) due to their capacity to provide stability, protection and resilience against natural disasters in coastal areas (Raihan et al., 2023) as well as a multitude of other ecosystem services (Barbier et al., 2011). Mangroves in the Gulf Cooperation Council (GCC) region, specifically *Avicennia marina* (gray mangrove; the dominant species) and *Rhizophora mucronata* (red mangrove) (Almahasheer, 2018), are often found as robust evergreen forest ecosystems widespread across the region despite the harsh environmental extremes such as highly variable temperatures and hypersalinity (Friis and Burt, 2020). Both species sustain themselves in their local environment due to their capability to adapt to higher salinity levels through genetic, physiological and morphological adaptations (Friis and Killilea, 2024; Shaltout et al., 2020). The total mangrove area in the GCC, while only representing a small fraction (0.11%) of the global mangrove extent of around 147,300 km^2, plays an outsized role in supporting biodiversity and ecological integrity in Saudi Arabia, UAE (United Arab Emirates), Qatar, Oman, Kuwait, and Bahrain (Friis and Killilea, 2024; Loughland et al., 2020; Bunting et al., 2022).

In the GCC countries, mangroves provide multiple ecosystem services with some specificities (Rondon et al., 2023), namely: a) water purification and filtration contributing to nutrient cycling, b) livelihood benefits such as pasture for camels and timber and wood for housing activities, c) protection against natural hazards such as high waves, flooding from storm surges, and coastal erosion, guaranteeing coastal shoreline stability, d) creating biodiversity hotspots by providing habitat for fisheries and other fauna (making this an important ecosystem for recreational and ecotourism activities) (Alsumaiti 2017; Mateos-Molina et al., 2021), and e) climate change mitigation through carbon sequestration (Lutz et al., 2011). This latter service is particularly critical, as mangroves function as carbon sinks (i.e. blue carbon) due to the significant storage potential (Donato et al., 2011). Carbon storage from mangroves has been estimated to be around 1200 tonnes of carbon per hectare (Elmahdy et al., 2020a) and at a global scale, mangroves are responsible for the sequestration of 25.5 million tonnes of carbon annually (Khader, 2023). This capacity is essential to the carbon-intensive economies of the GCC countries. Notably, in 2019, carbon emissions per capita in the GCC were among the highest globally. While the global average was 4.7 tCO_2e (carbon emissions in metric tons) per person, within Qatar it was 32.47 tCO_2e, and within the UAE it was 19.33 tCO_2e (Climate Watch, 2022). This highlights the potential of mangroves — if planted in optimal locations after considering climatic and anthropogenic factors – in offsetting emissions, in arid zones where freshwater is limited and other forest types are rare (Krauss et al., 2022).

Mangrove forests in the GCC are under pressure from a mix of natural and anthropogenic factors. In a recent study (Rondon et al., 2023) five main threats were identified: a) pollution from oil spills, sewage, and desalination plant operations, b) climate change-driven sea level rise and hypersalinity, c) coastal shoreline erosion and flooding, d) overexploitation of mangrove-resources such as for grazing or timber, and e) coastal development due to the rapid urban expansion in coastal areas. Natural disasters such as cyclones can also impact the regeneration dynamics of mangroves. Anthropogenic factors such as hydrological modifications, have affected mangroves negatively in Abu Dhabi (Alsumaiti and Shahid, 2019). The mangrove habitat establishment stage is highly influenced by various factors, including currents, water depth, wind, salinity, geomorphology, topography, tidal inundation, propagule predation, morphology, light, and nutrient availability (Otero et al., 2019).

A number of mangrove regeneration and restoration initiatives are being undertaken in the GCC region which aim to mitigate the impacts of climate change (Otero et al., 2019; Assaf et al., 2022; Burt and Bartholomew, 2019; Cougo et al., 2015; Leandro et al., 2022; Raihan et al., 2023). In Saudi Arabia, the restoration efforts on Al-Sharifa Island in the Red Sea have achieved a promising survival rate for planted *A. marina* saplings, which stood at 39% after 2 years, similar to the global average for the species (Chithambaran, 2019; Gorman et al., 2022). Saudi Aramco has established mangrove plantations along the Arabian Gulf and Red Sea coasts since 1993 and a mangrove eco-park in 2021 that conserves 64 km^2 of marine habitats (Aramco, 2023; Li et al., 2019). In the UAE, the Abu Dhabi National Oil Company (ADNOC), targets the future planting of 10 million mangrove trees as part of the UAE National Mangrove Planting Initiative (Morgan, 2023). The Abu Dhabi National Energy Company (TAQA) in its "Tree for 50″ campaign planted 50,000 new mangroves on Al Jubail Island in 2022 (Ismail and Hussein, 2022). Qatar has also taken some initiatives such as the establishment of the Al-Reem biosphere reserve in 2005, which includes mangrove habitats (Clüsener-Godt and Cárdenas Tomažič, 2016) and the planting and conservation mangrove program of Ras Laffan Industrial City in 2012 (Milani, 2018). In Kuwait, successful planting has occurred in Kuwait Bay and on the artificial islands of Sabah Al-Ahmad Sea City (Loughland et al., 2020). Previous attempts were made to establish mangrove plantations in Kuwait in the 1960s, but were unsuccessful (Firmin, 1968). In Oman, a partnership with the Japanese government has driven the planting of saplings in most of the governorates since 2000 (UNEP, 2018). In Bahrain, sea level rise presents a serious threat and mangrove restoration and regeneration are considered as important climate mitigation strategies.

Considering the fragility of mangrove forests and the recent interest in mangrove restoration activities in the GCC, it is of paramount importance to understand the climatic, anthropogenic, and environmental factors that influence mangrove forest health and growth in order to locate suitable areas for regeneration activities and optimize survival rates. The two objectives of this study were: i) to develop a mangrove forest regeneration age map – which represents the age of all the existing mangroves that were planted in the past 37 years. For this, long-term (1986–2023) Landsat satellite imagery and the random forest classification algorithm were used; and ii) to identify the underlying drivers that contribute to the successful afforestation of mangroves in the GCC region using logistic regression analysis. Our work holds potential to assist countries implement their afforestation and carbon sequestration goals in a resilient manner, and help enhance strategic planning and monitoring paradigms.

2. Methods

2.1. Study area

The GCC region (Fig. 1) has a subtropical climate with marked environmental extremes, usually characterized by highly variable and extreme temperatures with high salinities (Vaughan et al., 2019; Carvalho et al., 2019). The soil texture of this region is mostly either sandy, loamy sand or sandy loam (Bashour et al., 1983). The Gulf's climate, intensely tropical in summer and more temperate in winter, significantly influences the local biota, particularly mangroves. Mangrove species are limited by the occurrence of maximum temperatures (above 40 °C) – conditions beyond their tolerance over a long period can cause morphological and physiological changes (Friis and Burt, 2020; Almahasheer, 2019; Mafi-Gholami et al., 2020, 2021). The mangroves in the GCC are at their northern ecological distribution limits and can also be constrained by winter cold and hypersalinity. Salinity levels also vary across the region, with lagoons in the Arabian Gulf regularly exceeding 50 PSU (Practical Salinity Unit), and can reach over 70 PSU in tidal ponds (Burt and Paparella 2023). Qatar's ocean salinity ranges between 33 and 45 PSU (Rakib et al., 2021; Elobaid et al., 2022; Al-Ansari et al., 2022) and Saudi Arabia's Al-Kharrar Lagoon has an average of 40.5 PSU (Al-Dubai et al., 2017; Blanco-Sacristán et al., 2022). As mentioned earlier, the region is home to two mangrove species, *Avicennia marina* which grows naturally in all of the GCC countries (except Kuwait) and the less common *Rhizophora mucronata*, both well adapted to the extreme environmental conditions of high temperatures and hypersalinity (Almahasheer, 2018; Friis and Burt, 2020; Getzner and Islam, 2020; Rondon et al., 2023).

2.2. Data and preprocessing

2.2.1. Data sources

Landsat 5 Thematic Mapper (TM), 7 Enhanced Thematic Mapper (ETM+) and 8 Operational Land Imager (OLI) images were used to map mangroves in the GCC region from 1986 to 2023. These images provided consistent 30-m spatial resolution data, which allowed for the identification of mangrove cover through a combination of spectral bands particularly sensitive to vegetation. Five spectral bands namely Green, Red, Near Infrared (NIR), Shortwave Infrared 1 (SWIR1) and Shortwave Infrared 2 (SWIR2) were used. These spectral bands are represented as Band 3 (0.63–0.69 μm), 4 (0.77–0.90 μm), 5 (1.55–1.75 μm), and 7 (2.09–2.35 μm) in the Landsat 5 and 7 images and Band 4 (0.636–0.673 μm), 5 (0.851–0.879 μm), 6 (1.566–1.651 μm) and 7 (2.107–2.294 μm) in Landsat 8 images. These bands are optimal for detecting the unique spectral signatures of mangroves (Li et al., 2019). To maintain consistency in temporal analysis, the selection of imagery from both satellites was standardized to scenes with minimal cloud cover and during similar seasonal periods (July to December) to mitigate the impact of phenology on the spectral signature and to align data collection

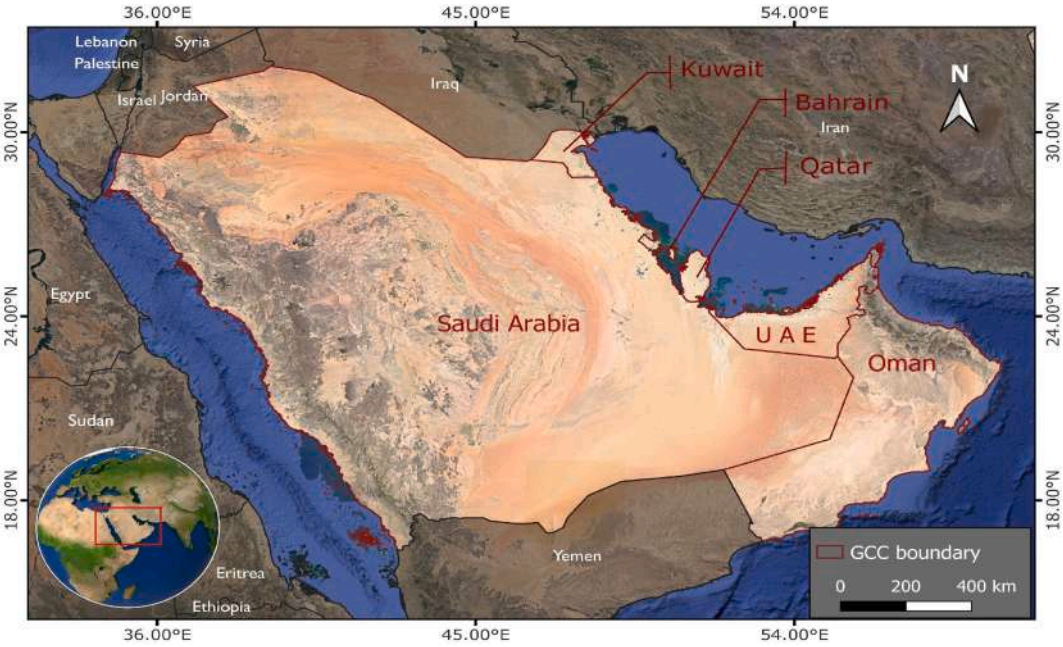

Fig. 1. Location of the study area GCC countries.

with the growing season of *Avicennia marina* (Hegazy, 1998). The GCC experiences mostly clear skies with cloud cover less than 10% during this period.

The 30-m resolution Advanced Land Observing Satellite Digital Surface Model (ALOS DSM) was also used to delineate mangrove ecosystems. Administrative boundaries, critical for defining the study area, were delineated using the global administrative areas (GADM) database (version 2.5, July 2015). The use of this dataset provided accurate administrative divisions, ensuring that the assessment of mangrove cover was confined to the geopolitical limits of the country members of the GCC (Yancho et al., 2020). In addition, data from the 30-m resolution Global Mangrove Watch (GMW) shapefile (Bunting et al., 2022) were used as a guide to show the extent of mangroves in the study area for the construction of mangrove bounding geometry. The coastal region of the GCC was used for this study by visually cross-referencing the mangrove areas in Google Earth Pro historical imagery and the Global Mangrove Watch 3.0 as references. A buffer area extending 10 km inland and 5 km seaward was applied for analysis.

2.2.2. Data pre-processing

The preparation of Collection 2 Level 2 Landsat 5, 7, and 8 datasets involved cloud masking, computation of various indices, image compositing, and masking based on elevation and index thresholds. All the spatial operations and analyses were performed in the Google Earth Engine (GEE) platform (Gorelick et al., 2017). The first step in pre-processing was cloud masking, which is critical for mitigating the impact of cloud cover and shadows on satellite imagery. Using the '*QA_PIXEL*' for Landsat datasets, a cloud masking function was applied. This function was vital for discerning vegetated regions within the imagery. By integrating temporal parameters to link the phenologically active season of *Avicennia marina* to the cloud masking algorithm, we ensured that only the reliable, cloud-free pixels were retained for analysis, as described by Mahamunkar et al. (2022). A gap filling algorithm was also used to mask the Landsat 7 ETM + scan line corrector (SLC) error.

Subsequently, we calculated 7 spectral indices commonly used for mangrove identification. These indices included: 1) the normalized difference vegetation index (NDVI); utilizes the reflectance of Red and Near-Infrared (NIR) bands to indicate vegetation health based on chlorophyll content; the index values range between −1.0 and + 1.0, with high positive values indicating healthy and dense vegetation (Gupta et al., 2018; Hereher and Al-Awadhi, 2019; Mohanty et al., 2023; Nardin et al., 2016; Habibullah et al., 2022; Phong and Nuong, 2023); 2) the modified normalized difference water index (MNDWI); uses Green and ShortWave InfraRed (SWIR) bands to maximize the reflectance from water bodies and minimize land noise, effectively delineating water from land (Hickey and Radford, 2022; Habibullah et al., 2022; Sahadevan et al., 2021); 3) the normalized difference mangrove index (NDMI); designed to highlight the spectral differences between mangrove forests and terrestrial vegetation by comparing the reflectance in the Green and SWIR bands (Habibullah et al., 2022); 4) the simple ratio (SR) (Elmahdy et al., 2020b; Yancho et al., 2020); 5) Band Ratio 54; 6) Band Ratio 35; and 7) the Green Chlorophyll Vegetation Index (GCVI), a vegetation index sensitive to chlorophyll content (Table 1).

A composite image of the Landsat imagery was then created using the "median reducer". The masking process was dual-faceted. First, the ALOS DSM was utilized to mask areas above 30 m and below −5 m in elevation to mean sea level, as mangroves typically occur at lower elevations (Bunting et al., 2018). Previously, remote sensing-based studies from around the globe have used similar height thresholding to exclude areas that can not be mangroves and reduce the number of pixels without mangroves that could be misclassified (Fatoyinbo et al., 2008; Simard et al., 2019; Cissell et al., 2021). Then, the computed NDVI values were used to further

Table 1
Spectral indices used for mangrove identification; adapted from Oliver et al. (2022).

Index	Equation	Target	Reference
Normalized Difference Vegetation Index (NDVI)	(NIR - Red)/(NIR + Red)	Vegetation	Mohanty et al. (2023)
Normalized Difference Mangrove Index (NDMI)	(SWIR 2 - Green)/(SWIR 2 + Green)	Mangrove identification	Habibullah et al. (2022)
Modified Normalized Difference Water Index (MNDWI)	(Green - SWIR 1)/(Green + SWIR 1)	Water information	Habibullah et al. (2022)
Simple Ratio (SR)	NIR/Red	Simple vegetation index	Gupta et al. (2018)
Band Ratio 54	SWIR1/NIR	Water features	Oliver et al. (2022)
Band Ratio 35	Red/SWIR 1	Water features	Oliver et al. (2022)
Green Chlorophyll Vegetation Index (GCVI)	(NIR/Green) - 1	Greenleaf biomass	Habibullah et al. (2022)

refine the mask. Areas with an NDVI less than 0.15 were assumed to be devoid of mangroves. To determine the specific thresholds, we overlaid the GMW 2020 raster layer onto the DSM and NDVI layers for the entire coastal GCC region and extracted random samples across this area to identify the appropriate threshold values. The main steps and the approach used, including the mangrove mapping (input data), yearly mangrove classification, and yearly mangrove loss and gain used to construct the secondary mangrove forest age map are shown in Fig. 2.

2.3. Mangrove classification

2.3.1. Training data preparation

Training data was collected across the entire coastal region of GCC using Google Earth Pro. The focus was on identifying pixels that were temporally stable. High-quality satellite images are available from 2001 to 2023 in certain areas of the GCC, and these images were screened manually to find only those areas that remained stable over time. These stable areas were then utilized as training samples for land cover classifications. The main land cover classes were ‘mangroves’, ‘non-mangrove vegetation’, and ‘agriculture’. All non-vegetation land covers such as roads, built-up areas, water bodies and barren land were amalgamated as ‘others’. After collection, the data was split into 2 parts for model validation, that included 70% for training and 30% for validation (Table 2 and Fig. 3).

2.3.2. Model fitting

In this study, the Random Forest (RF) algorithm was used for the classification. Random forest is an ensemble learning method that creates a collection of decision trees during training. Each tree in the forest is built from a sample drawn with a replacement (bootstrap sample) from the training set, and split decisions are made at each node based on a random subset of these features. This approach enhances diversity among the trees, which reduces overfitting and improves generalization to unseen data. The final classification decision is made based on the majority voting principle, where the class label predicted by the majority of the trees is chosen as the final output, thereby enhancing the accuracy and robustness of the model (Breiman, 2001; Jamaluddin et al., 2022). The training process of the random forest was conducted on the GEE platform. The RF classification algorithm has been extensively employed in mangrove mapping and classification studies (Diniz et al., 2019; Jamaluddin et al., 2022). This widespread usage of RF for its robustness against overfitting and outliers influenced our decision to select it as the classification algorithm for our study (Mahamunkar et al., 2022).

The *.smileRandomForest* classifier in Google Earth Engine was applied to the selected bands and landcover properties. Separate RF models were fitted to each country for each year. The 6 variables shown in Table 1 were used in the model training. The RF algorithms were trained using 70% of the samples collected to calculate the overall accuracy, F1-score of mangroves class and the Cohen's kappa coefficient of the overall classification result. The F1-score was derived from the confusion matrices. The kappa statistic provides a measure of how well the classification performed compared to random chance, with values above 0.8 (up to 1) indicating good predictive power (Hickey and Radford, 2022). The F1-score is the harmonic mean of precision and recall and is a useful metric for unbalanced datasets, as it accounts for both false positives and false negatives. Values for the F1-score range from 0 to 1 and categories of 0.5–0.7, 0.7 to 0.8, 0.8 to 0.9, and >0.9 can be classified as poor, acceptable, excellent, and outstanding discrimination, respectively.

Since the training data was temporally stable, the same training samples were used to classify the maps of each year. Hyperparameter tuning was initially done using the data for the year 2023 for the four model parameters, namely number of trees, variables per split, minimum leaf nodes, and bagging fraction, and their values were used for the remaining models. To fine-tune these parameters, we conducted a grid search over a range of values for each parameter and evaluated the performance based on the kappa coefficient. For the number of trees, we tested values ranging from 10 to 100, and for variables per split, we tested values from 1 to 5. The parameters of 20 decision trees and 3 randomly selected predictors per split were considered to ensure a robust and unbiased classification with higher kappa coefficient. Varying other parameters such as the bagging fraction from 0.5 to 1.0 showed little differences in performance, suggesting that the default value was sufficient. Similarly, the minimum leaf nodes parameter had no significant effect on the kappa coefficient, so its default value was retained to reduce model complexity and avoid overfitting. The RF algorithm employed majority voting to determine the final predicted result from each tree. For the classified maps, a masking technique, using pixel count, was utilized to filter out the noise and unconnected pixels, thus enhancing the clarity and accuracy of the classified image, which is a critical step for producing a clean and interpretable map of the results (Mahamunkar et al., 2022). Hence, as a step to reduce noise in the classified mangrove maps, all mangrove pixels connected to 4 or less similar pixels were considered to be too low and were masked out. The final result from the RF algorithm is mangrove cover maps of the study area from 1986 to 2023.

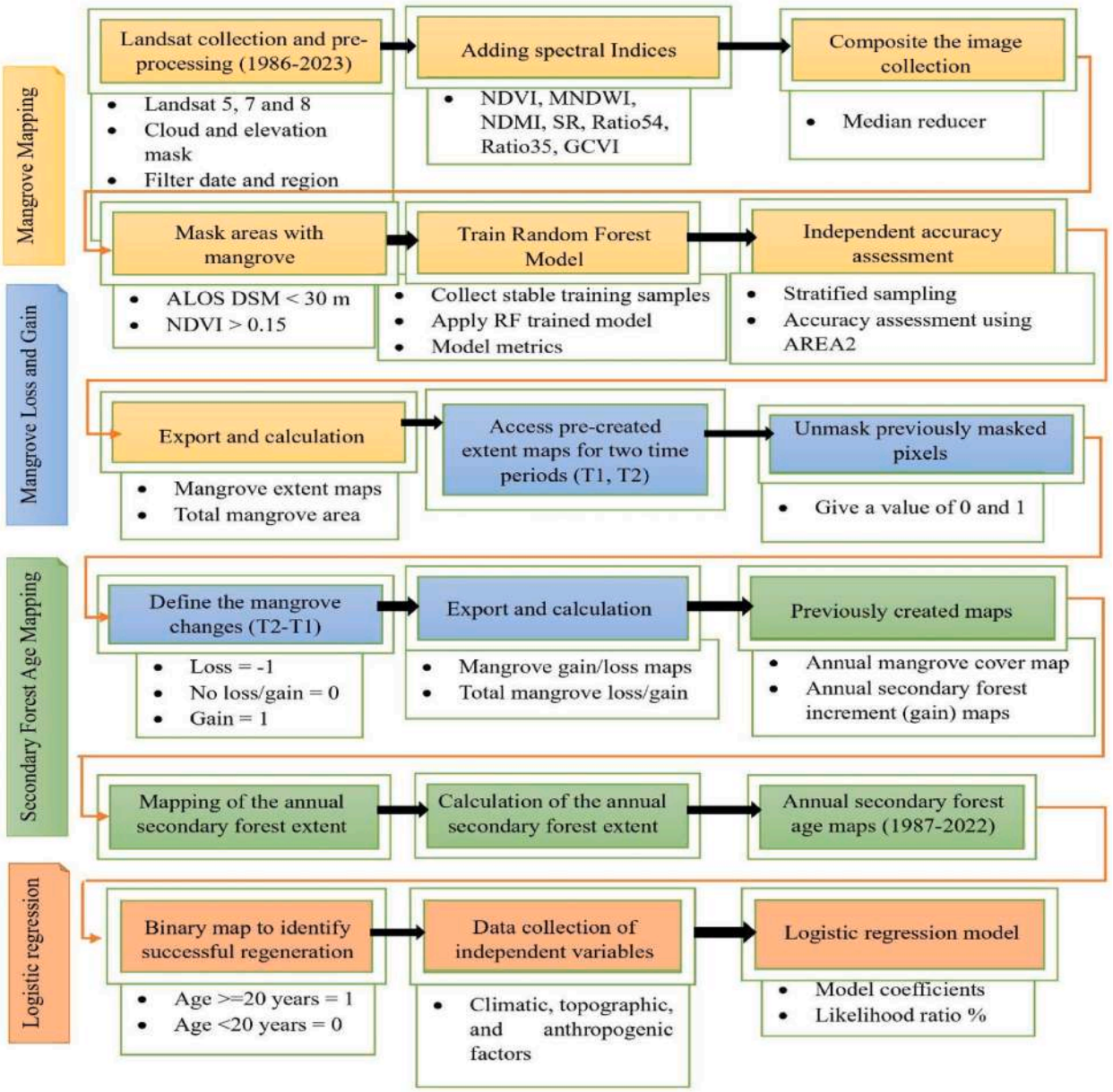

Fig. 2. Flowchart showing the main steps and the approach used(T2 here represents the year of focus and T1 is the year before that).

Table 2
Number of samples used in the training and validation dataset.

Class	Training samples	Validation samples
Mangrove	9289	2384
Non-mangrove vegetation	1430	613
Agriculture	239	103
Others	2473	1060

2.3.3. Independent accuracy assessment

Classified mangrove maps at equal intervals of five years starting from 2003 to 2023, were subjected to a stratified sampling for independent accuracy assessment using the AREA2 (Area Estimation & Accuracy Assessment) framework developed using the principles of Olofsson et al. (2014). The classified mangroves were then matched with high resolution historical images in Google Earth Pro. The AREA2 framework was then used for calculating the mangrove producer's accuracy, user's accuracy, and mangrove area at ± 95% confidence interval.

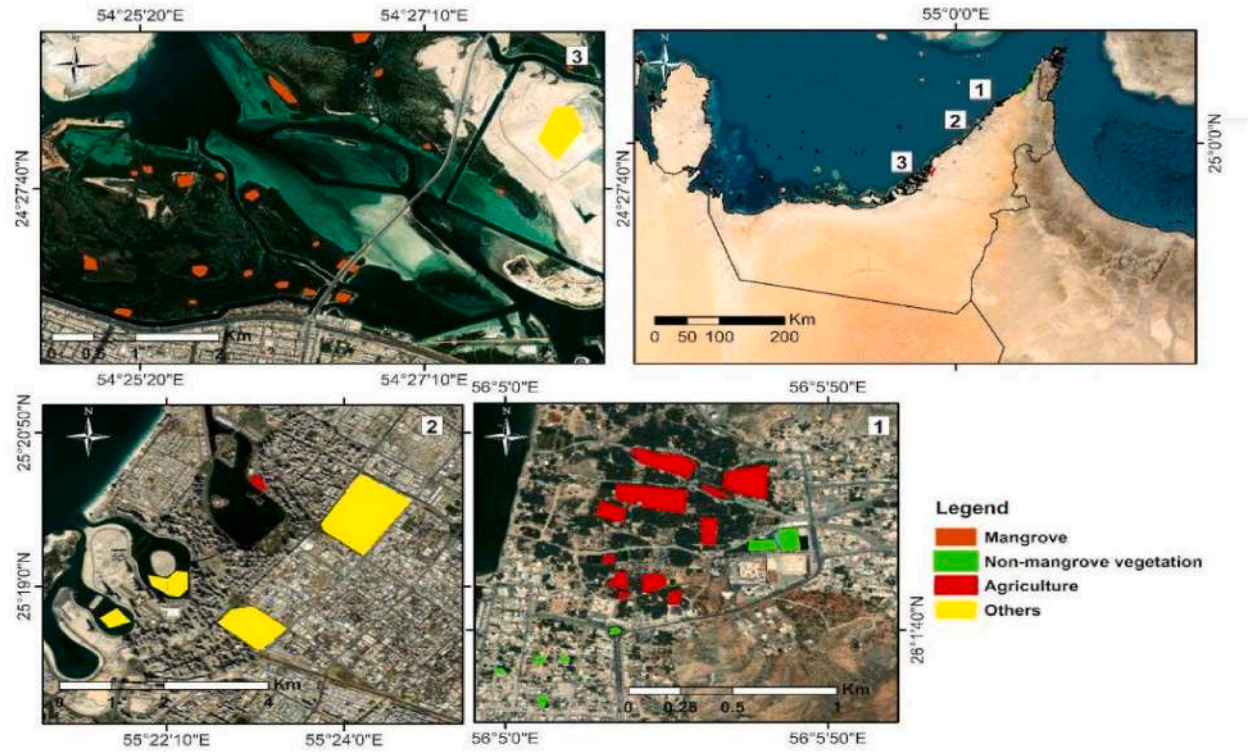

Fig. 3. Distribution of training data (Orange: Mangrove, Green: Non-mangrove vegetation, Red: Agriculture, Yellow: Others). (For interpretation of the references to colour in this figure legend, the reader is referred to the Web version of this article.)

2.4. Secondary mangrove forest age mapping

The previously determined extent of mangrove cover and annual mangrove gain for the studied period constitute the main input datasets to generate the secondary mangrove age maps, which will provide a clear understanding of the mangrove growth dynamic. Changes in mangrove area were determined as annual differences in area between maps (Silva Junior et al., 2020). This method involves determining changes by subtracting two pairs of mangrove cover extents from two consecutive years (i.e. next year extent (Y_i+1) minus the preceding year (Y_i)). The first step consisted of selecting two different maps of mangrove cover for two consecutive time periods, after which the previously non-mangrove masked pixels were reclassified as 0 value to facilitate the mathematical operation. Change maps are then produced by calculating the difference between (Y_i+1) and (Y_i). The resulting change has been categorized into −1, 0 and 1 representing mangrove loss, no change and mangrove gain, respectively. This operation was carried out for each successive year until complete maps of mangrove dynamics were obtained. A total of 36 mangrove gain maps were produced and exported for further analysis, serving as input for secondary age maps within R software.

For generating annual maps depicting the secondary mangrove forest extent in the year *i*, binary mangrove gains were created by assigning values of 0 and 1 for the non mangrove and mangrove pixels, respectively. These maps were then accumulated up to the designated year starting from 1986 (equation (1)). Given that this sequential summation may result in values up to 37, the resultant secondary mangrove extent maps were binarized by assigning "1" to pixels with values greater than 1, and the remaining 0 pixels were kept unchanged. They were subsequently, multiplied by their respective binary cover extent to eliminate mangrove gain pixels from the previous year that were deforested in the year *i* as calculated through equation (2). The final map contains all secondary mangrove forest pixels from the years *i* and *i-1*.

$$E_i = \sum_{Y_1}^{Y_i} G_i \tag{1}$$

$$X_i = E_{ri} Z_i \tag{2}$$

Where, G_i is the binary mangrove gain map in the year *i*, E_{ri} is the reclassified total annual secondary mangrove forest extent and Z_i corresponds to the binary mangrove forest cover extent map in the year *i*, with the units for *E*, *G*, *X* and *Z* in number of pixels.

The cumulative summation of the binary final secondary forest maps represents the annual secondary forest age maps for the year in question. This metric (i.e., age maps) corresponds to the number of years since a pixel, initially classified as non-mangrove, transitioned to a pixel representing mangrove cover, indicating mangrove gain. The 2023 age map was then determined through a year-by-year summation of the age of secondary forests beginning from 1987, where the first mangrove gains were detected in the first transi-

tion (1986–1987) (See equation (3)). Deforested secondary mangrove forests were removed from each age map by multiplying with the binary mangrove forest cover map. The values of each pixel in 2023 represent the age of the pixels having a value between 1 and 37.

$$Asf_{1986} = 1\ year\ old\ map\ Asf_{1987} = \left(Asf_{1986} + X_{1987}\right) Z_{1987}\ Asf_{1988} = \left(Asf_{1987} + X_{1988}\right) Z_{1988}\ \ldots\ldots Asf_i = \left(Asf_{i-1} + X_i\right) Z_i \quad (3)$$

Where, Asf_i is the age of secondary mangrove forest map in the year i, X_i is the annual secondary mangrove forest extent binary map in the year i and Z_i corresponds to the mangrove forest cover extent binary map in the year i, with the units for X and Z in number of pixels. See Fig. 4 for details.

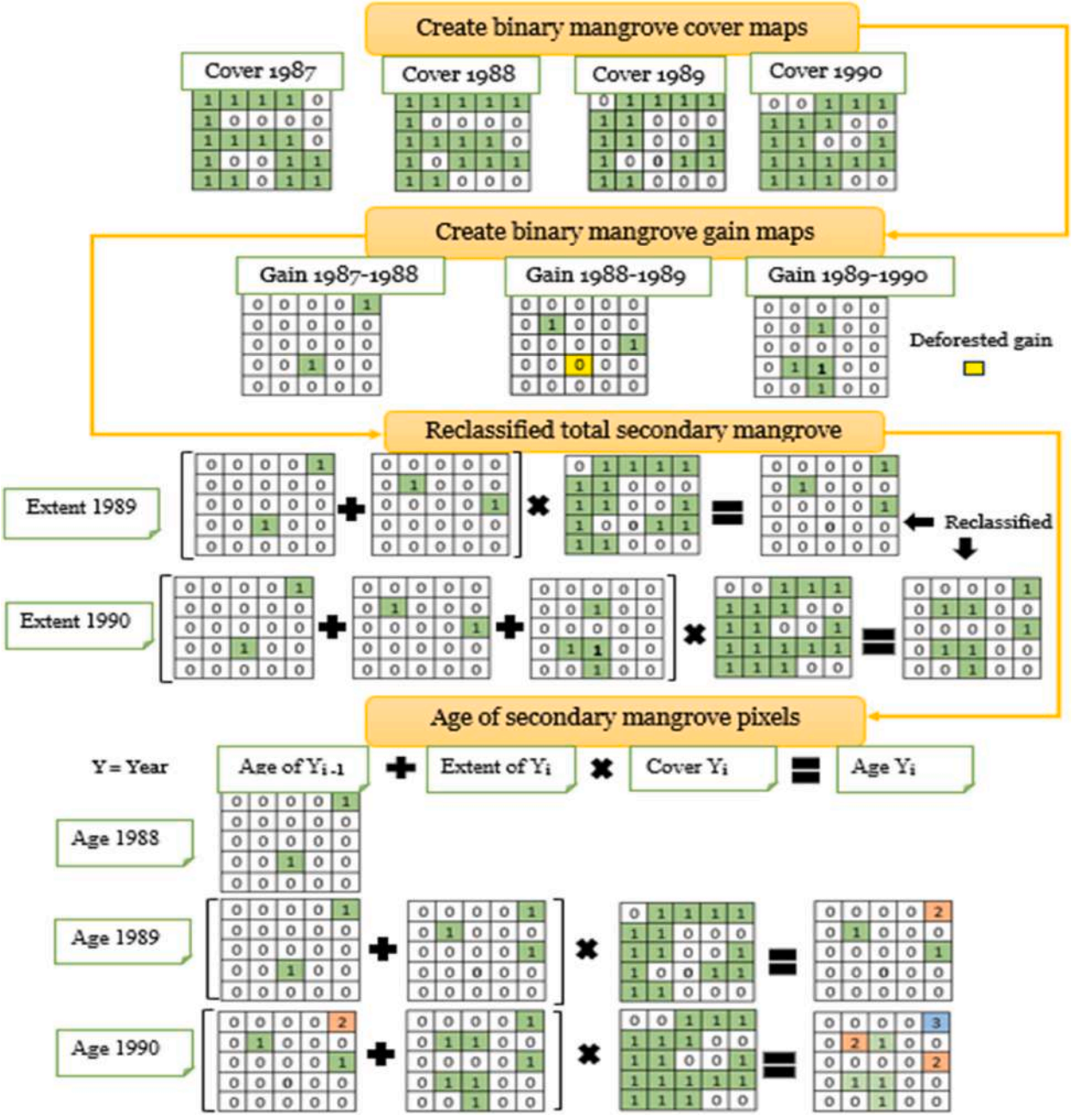

Fig. 4. Diagram showing the steps related to annual gain-loss products and secondary forest age map generation.

2.5. Logistic regression analysis

Logistic regression was used to determine the drivers of mangrove growth in the GCC region. All mangrove pixels in the age map occurring after 1986 and having age greater than 20 years were considered old enough to be used as a proxy for successful regeneration (Sillanpää et al., 2017). We then extracted two groups of pixels within our areas of interest using simple random sampling. The first group represents areas where secondary mangroves age are greater than 20 years that denote successful growth; the second group represents areas with no mangrove forest (which were in close proximity to areas with mangroves). For both groups 10,000 pixels were taken in order to determine the drivers of mangrove forest regeneration success in the GCC region. Since the outcomes were binary i.e., presence or absence of regenerating mangroves, we used logistic regression to investigate the existing correlations between a dichotomous dependent variable (1 = mangrove forest presence and 0 = mangrove forest absence) and the independent variables. We selected two important groups for the independent variables: environmental and anthropogenic factors (Petrosian et al., 2016; Pir Bavaghar, 2015) (Table 3). Different spatial datasets were acquired and used as independent variables including the NASA SRTM DEM, MODIS LST, CHIRPS rainfall data, OpenLandMap Soil data, and the Copernicus LULC datasets (Nguyen, 2019). The selection of the explanatory variables used in the logistic regression was based on available variables that have been previously used in similar studies in other regions to study mangroves (Pham and Yoshino 2016; Petrosian et al., 2016).

The NASA SRTM DEM is a digital elevation model that provides an estimate of global elevation to the mean sea level at 30 m spatial resolution. The MODIS (Moderate Resolution Imaging Spectroradiometer) LST (Land Surface Temperature) provides daily temperature data retrieved at 1 km native spatial resolution, which was used to estimate the median, maximum and minimum temperature for the past 10-year period. The Climate Hazards Group InfraRed Precipitation with Station data (CHIRPS) is a global rainfall data set ranging from 1981 to near-present. The OpenLandMap Soil data provides a global soil map including soil pH and soil moisture at different depths and has a 250 m native spatial resolution. The Copernicus LULC (land use and land cover), the GHS Settlement Characteristics, and the WorldPop population density datasets provided insight into the different anthropogenic factors being studied.

The stepwise regression method was used to identify the set of most suitable variables and their potential interaction with each other to increase the efficiency of the model in terms of AIC (Akaike Information Criterion), a metric that aids in model selection. Generally, lower AIC values are associated with better model performance. After selecting the best model, McFadden's Pseudo R^2 was calculated to assess the goodness-of-fit by quantifying model improvement using the ratio of the log-likelihood of the model to log-likelihood of the null model. The value of McFadden's Pseudo R^2 ranges between 0 and 1, with values closer to 1 considered to be a better model fit. The associated chi-square statistic of the stepwise logistic model, which evaluates the significance of the model by comparing it with a null model, was also calculated. The calculations for logistic regression were done using the R statistical software version 4.2.2 (R Core Team, 2022).

The regression model used in this study is specified in the following equation:

Table 3
Independent variables that were considered for selection in the logistic regression model.

Category	Variable	label	Unit	Source
Environmental	Elevation	E1	Meters	Jarvis et al. (2008)
	Slope	E2	Percentage	Jarvis et al. (2008)
	Minimum temperature	E3	Celsius	Wan et al. (2021)
	Mean temperature	E4	Celsius	Wan et al. (2021)
	Maximum temperature	E5	Celsius	Wan et al. (2021)
	Mean precipitation	E6	Millimeters	Funk et al. (2015)
	Maximum precipitation	E7	Millimeters	Funk et al. (2015)
	Soil pH at depth 0 m	E8	–	Hengl (2018)
	Soil pH at depth 30 cm	E9	–	Hengl (2018)
	Soil moisture at depth 0 m	E10	Liters	Hengl and Gupta (2019)
	Soil moisture at depth 30 cm	E11	Liters	Hengl and Gupta (2019)
	Distance from river	E12	Meters	Buchhorn et al. (2020)
	Elevation x Slope	E1 x E2	–	Jarvis et al. (2008)
	Minimum temperature x Mean precipitation	E3 x E6	–	Wan et al. (2021); Funk et al. (2015)
	Mean temperature x Mean precipitation	E4 x E6	–	Wan et al. (2021); Funk et al. (2015)
Anthropogenic	Population density	A1	–	WorldPop (2020)
	Distance from agricultural areas	A2	Meters	Van Tricht et al. (2023)
	Distance from roads	A3	Meters	Pesaresi and Politis (2023)
	Distance from urban areas	A4	Meters	Buchhorn et al. (2020)
	Population density x Distance from agricultural areas	A1 x A2	–	WorldPop (2020); Van Tricht et al. (2023)
	Population density x Distance from urban areas	A1 x A4	–	WorldPop (2020); Buchhorn et al. (2020)
	Distance from agricultural areas x Distance from urban areas	A2 x A4	–	WorldPop (2020); Van Tricht et al. (2023); Buchhorn et al. (2020)

$$p = E(Y) = \frac{exp\left(\beta_0 + \beta_1 x_1 + \beta_2 x_2 + \ldots + \beta_i x_i + \beta_j x_1 * x_2\right)}{1 + exp\left(\beta_0 + \beta_1 x_1 + \beta_2 x_2 + \ldots + \beta_i x_i + \beta_j x_1 * x_2\right)} \quad (4)$$

Where, p is the probability of mangrove occurrence ($0 \leq p \leq 1$), E(Y) – expected value of the binary dependent variable Y, β0 – constant to be estimated, βi – predicted coefficient of each independent variable Xi. The last term $\beta_j x_1 * x_2$, is a simple representation of the interaction effects tested. The amount of the contribution of each factor to mangrove occurrence is described by the regression coefficient (Pir Bavaghar, 2015). Independent variables X*i* with a high contribution to mangrove occurrence and statistically significant p-values ($\alpha < 0.05$) in the samples of areas where mangroves age is greater than 20 years were identified. Thus, based on the set of independent variables, the maximum likelihood estimation was applied to estimate the probability of occurrence of successful mangrove regeneration in the future (Pham and Yoshino, 2016; Pir Bavaghar, 2015).

3. Results

3.1. Accuracy assessment of the mangrove cover in the GCC

The accuracy assessment for mangrove cover classification using the random forest model across the GCC countries was conducted for the study period (1986–2023). The F1-score for mangroves and the kappa coefficient of the overall classification were generated based on the confusion matrix to assess the mangrove classification accuracy from landsat data using 30% validation data of the total collected samples. Table 4 shows the Kappa coefficients and the F1-score of mangrove extent in the GCC countries (1986–2023). The results demonstrate a consistently high level of accuracy throughout the studied period (Gilani et al., 2021; Hickey and Radford, 2022).

In Saudi Arabia, the F1-score of mangrove cover classification ranged between 0.9 and 0.95; Kappa coefficient values indicated agreement, ranging from 0.73 to 0.96 over the study period. In the United Arab Emirates (UAE), the F1-score ranged from 0.92 to 0.97 and Kappa between 0.83 and 0.97. For Qatar, the F1-score was between 0.86 and 0.91, with Kappa ranging from 0.74 to 0.87. Similarly, Oman and Bahrain also exhibited high F1-scores, generally maintaining values above 0.89. The kappa coefficients in these countries indicated strong agreement ranging between 0.84 and 0.98. The user (UA) and producer accuracy (PA) values for all countries and classifications ranged between 0.7 and 1.

An independent accuracy assessment was also undertaken using stratified sampling and Google Earth Pro high-resolution historical images (2003–2023) to provide validation for the mangrove classification and model performance. The producer's accuracy (PA), user's accuracy (UA) and the 95% confidence interval for mangrove area is given in Table 5. The values of UA were generally found to be higher than that of PA, indicating that there were relatively fewer false positives for identified mangroves than false negatives. We did not conduct an independent accuracy assessment for Kuwait due to a lack of any mangroves in the earlier years, and significantly fewer mangrove areas were identified compared to the other countries (see Table 6).

3.2. Mangrove area results

The spatiotemporal distribution of mangrove extent in GCC countries during the 1986–2023 period was predicted from the Random Forest (RF) classification. The results at five-year intervals are presented in Table 6.

The findings reveal a notable increase in mangrove cover across the GCC regions over the 37-year period (Fig. 5). The total mangrove area in the GCC has more than doubled from 1986 to 2023. The United Arab Emirates (UAE) demonstrated the highest percentage of mangrove cover in the region, alone exceeding 50% mangrove cover during all time periods. Even in terms of absolute area, the UAE has increased its mangrove cover by almost 150% in the last 37 years. Saudi Arabia has also witnessed a substantial rise, with mangrove cover growing from 2302 ha in 1986 to 6295 ha in 2022. Notably, between 2018 and 2023, a remarkable growth of 1327 ha has occurred, representing a substantial 27% increase in just five years. Saudi Arabia's contribution to the overall GCC mangrove extent is significant, constituting 40% of the total GCC mangrove area in 2023.

Qatar has also seen an exponential positive growth in mangrove area, from only 27 ha of mangroves in 1986 to 554 ha in 2023, which is a 21-fold increase. In Oman, there was a decline in mangrove area, from 605 ha in 1986 to 189 ha in 2023, providing evi-

Table 4
Accuracy assessment of mangrove extent in the GCC countries for selected years from 1986 to 2023.

Country	F1-score and Kappa	1986	1993	1998	2003	2008	2013	2018	2023
Saudi Arabia	Mangrove F1-score	0.92	0.93	0.96	0.95	0.95	0.91	0.90	0.90
	Kappa	0.91	0.96	0.96	0.86	0.91	0.80	0.79	0.73
UAE	Mangrove F1-score	0.97	0.95	0.91	0.92	0.92	0.92	0.93	0.96
	Kappa	0.97	0.97	0.91	0.92	0.98	0.83	0.92	0.94
Qatar	Mangrove F1-score	0.90	0.89	0.90	0.87	0.91	0.90	0.88	0.86
	Kappa	0.72	0.84	0.78	0.83	0.87	0.86	0.79	0.81
Oman	Mangrove F1-score	0.96	0.91	0.91	0.89	0.96	0.99	0.95	0.97
	Kappa	0.87	0.92	0.92	0.93	0.84	0.98	0.93	0.94
Bahrain	Mangrove F1-score	0.90	0.96	0.93	0.97	0.97	0.96	0.98	0.98
	Kappa	0.90	0.95	0.94	0.97	0.97	0.95	0.98	0.98
Kuwait	Mangrove F1-score	–	–	–	–	–	0.76	0.78	0.78
	Kappa	–	–	–	–	–	0.75	0.78	0.78

Table 5
Independent accuracy assessment of mangrove extent in the GCC countries for selected years from 2003 to 2023.

Country	Assessment metrics	2003	2008	2013	2018	2023
Saudi Arabia	Mangrove PA	0.75	0.81	0.78	0.83	0.85
	Mangrove UA	0.87	0.90	0.89	0.88	0.91
	95% CI of area (ha)	1225.6	25.9	2543.2	1592.4	2308.2
UAE	Mangrove PA	0.79	0.79	0.82	0.78	0.78
	Mangrove UA	0.80	0.80	0.93	0.93	0.90
	95% CI of area (ha)	2025.2	2720.3	2405.8	2301.0	2491.4
Qatar	Mangrove PA	0.78	0.87	0.72	0.88	0.72
	Mangrove UA	0.85	0.93	0.94	0.95	0.93
	95% CI of area (ha)	257.9	140.4	144.8	341.0	423.8
Oman	Mangrove PA	0.75	0.80	0.73	0.81	0.78
	Mangrove UA	0.80	0.88	0.80	0.81	0.85
	95% CI of area (ha)	55.1	24.38	61.3	42.9	27.7
Bahrain	Mangrove PA	0.73	0.80	0.79	0.78	0.81
	Mangrove UA	0.82	0.89	0.81	0.85	0.88
	95% CI of area (ha)	10.9	19.6	10.3	16.2	13.4

Table 6
Mangrove cover predicted from the Random Forest classification model at five-year intervals (1986–2023) across the GCC countries.

Location	Mangrove extent	1986	1993	1998	2003	2008	2013	2018	2023
Saudi Arabia	Area (ha)	2302	2685	3752	4624	3482	4089	4968	6294
	% of GCC mangrove	36.3	37.7	38.4	39.5	33.2	39.1	42.2	40.9
UAE	Area (ha)	3365	3916	5636	6475	6261	5705	6061	8313
	% of GCC mangrove	53.1	54.9	57.7	55.4	59.7	54.6	51.5	54.1
Qatar	Area (ha)	26.9	70.0	225	435	569	459	537	554
	% of GCC mangrove	0.4	0.9	2.3	3.7	5.4	4.4	4.6	3.6
Oman	Area (ha)	605	421	110	118	135	158	154	189
	% of GCC mangrove	9.6	5.9	1.1	1.0	1.3	1.5	1.3	1.2
Bahrain	Area (ha)	32.6	30.3	35.7	27.7	25.9	23.8	39.8	30.4
	% of GCC mangrove	0.5	0.4	0.4	0.2	0.2	0.2	0.3	0.2
Kuwait	Area (ha)	0.0	0.0	0.0	0.0	0.0	13.6	5.6	25.4
	% of GCC mangrove	0.0	0.0	0.0	0.0	0.0	0.1	0.1	0.2
Total mangrove area GCC (ha)		6331	7123	9760	11681	10474	10450	11765	15407

dence of mangrove deforestation in the country. However, there has been a steady increase in mangrove area in the recent past, with a 60% increase in the past two decades from 2003 to 2023, although the total area is still low relative to pre-2000s levels. In Bahrain, there was a modest change in mangrove cover, from 32 ha in 1986 to 30 ha in 2023, with a slight fall of 6% in recent years. Information on Kuwait was not included in the figure given that the total mangrove area was minimal.

Fig. 6 shows the temporal dynamics of mangrove cover around Abu Dhabi in the Persian-Arabian Gulf.

3.3. Mangrove cover change and secondary mangrove forest age map for 2022

3.3.1. Mangrove cover change

Saudi Arabia exhibited a net gain in mangrove cover throughout the time period. The greatest net gain occurred from 2017 to 2022, with an average gain of 837 ha per year. In the UAE, the period from 1992 to 1997 saw the most significant net gain, with mangroves expanding by 319 ha per year. Qatar's average mangrove cover gain for the whole period was 54.8 ha per year. Oman's data indicate variable trends, with periods of both loss and gain. Bahrain's mangrove cover changes were minimal and more stable compared to other GCC countries. Overall, the GCC experienced a substantial gain in mangrove cover, particularly in the last decade (2013–2023), where a net average gain of 86.4 ha per year was observed (see Figs. 7 and 8).

3.3.2. Secondary mangrove forest age map for 2022

The approach described in section 2.4 was used to estimate the age of secondary mangrove forest in the GCC region (See Fig. 9). Overall, 8.5% of secondary mangrove forest in GCC region (excluding Kuwait) are older than 30 years, which represents a mangrove extent of 420 ha. The youngest mangrove forests in the GCC, with ages less than 5 years, cover an area of 2036 ha (41.3 %) (See Fig. 9 A,B). Saudi Arabia and Oman possess the highest percentages of the youngest mangroves which constitute 70.4% (equivalent to 1616 ha) and 35.2% (72.3 ha), of their respective mangrove area. Meanwhile, the oldest secondary mangrove forests, where age is greater than 30 years old, are mainly found in Bahrain, constituting 38.5% of its total secondary mangrove area and a high percentage (19.5%) within this age class is also found in Qatar. Additionally, the 25-30 year-old secondary mangroves are notably concentrated in Qatar and Bahrain, where they account for 29.5% and 30.3% of their total mangrove area, respectively. The UAE has, however, a different mangrove age distribution, with the 10–15 years old being the most prevalent comprising 21.4 % of its mangrove area, followed by the 5 to 10 class that constitutes 17.5% of the area.

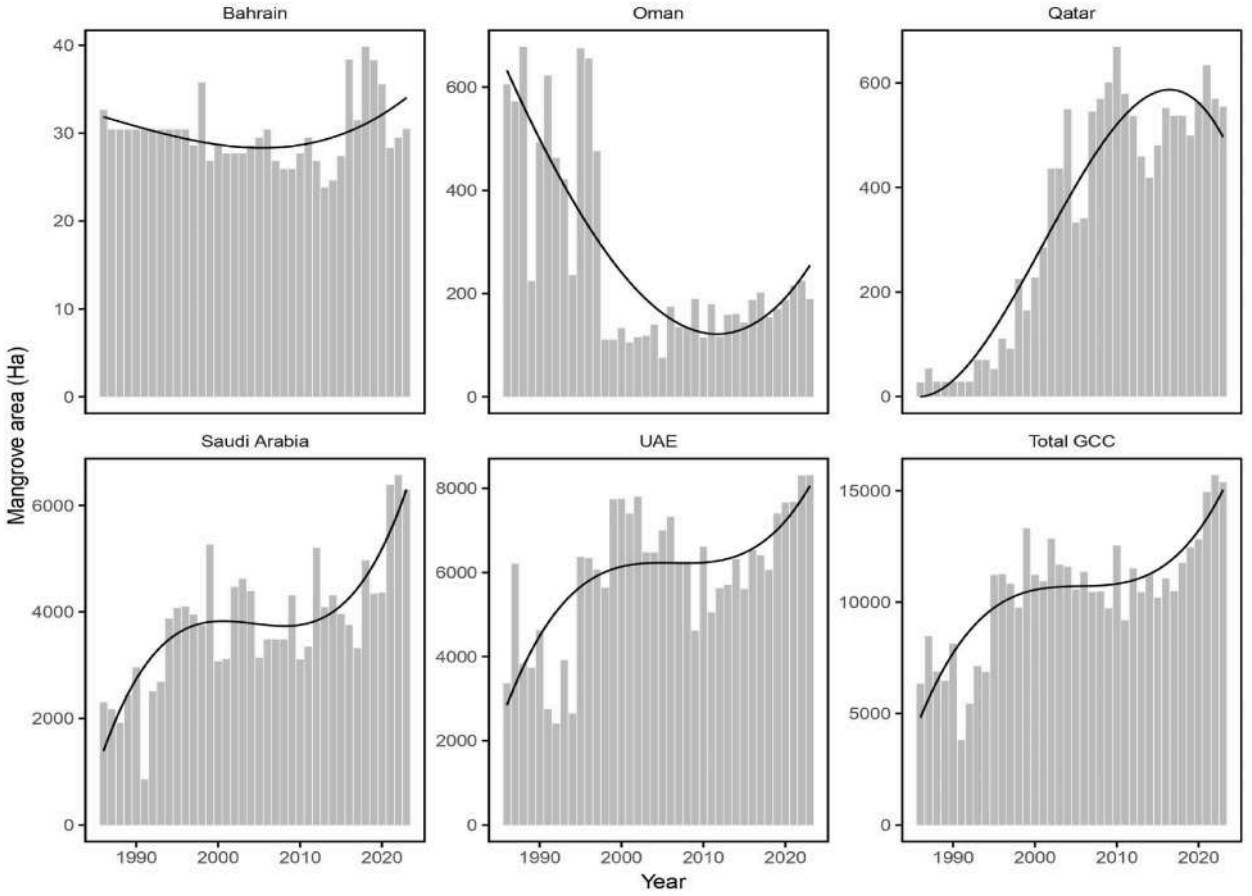

Fig. 5. Temporal trends in mangrove cover area in GCC countries from 1986 to 2023. Note differences in the y-axis scale between countries.

Fig. 10 shows the distribution of mangrove ages in the GCC. In the UAE, the youngest mangroves, falling within the age class of 0–15 years, are predominantly situated in Abu Dhabi, Dubai, and Ajman. The older mangrove stands, exceeding 15 years in age, are primarily concentrated in Umm Al Quwain and Ras Al Khaimah. In Saudi Arabia, mangroves exhibit a mixed age composition, with notable concentrations in Makkah, Ash Sharqiya, and the Jizan region. In Qatar, the younger mangroves thrive in Al Ruwais, while the older mangroves can be found in Al Khor. It is noteworthy that Al Khor consists of both the oldest and youngest mangroves within the country. In Oman, the distribution of mangrove age is dispersed, and has both younger and older mangroves. However, in Al Wusta, most of the mangroves are old, whereas in Muscat and Ash Sharqiyah South, younger aged forests are present. Lastly, in Bahrain, mangroves of varying ages are primarily concentrated in the central regions. This indicates a diverse age composition within the mangrove population across the country.

3.4. Logistic regression analysis

The results showed that a large number of factors, both environmental and anthropogenic, contributed to the success of afforestation and regeneration of the mangroves of the UAE between 2001 and 2022. We used a stepwise regression method to eliminate the statistically non-significant variables. The stepwise model performed marginally better (AIC = 3101) than the original logistic regression (AIC = 3108) in terms of model simplicity. The stepwise regression analysis provided a means of identifying the most important factors and their interaction terms that influence the success of regeneration in the GCC. The regression coefficients within the model show both the direction and level of the impact of independent variables on the likelihood of mangrove regeneration (see Table 7). Out of the 16 originally evaluated independent variables and 6 interaction terms, 9 variables and 4 interaction terms were found to be statistically significant at the 95% confidence level through the stepwise regression process (See equation (5)). The McFadden's Pseudo R^2 for the final model was 0.38, indicating the model is a good fit for predicting secondary mangrove regeneration. The associated p-value of the chi-square test also showed a high level of significance at close to 0 (chi-square value = 1907.26, df = 20).

Among the environmental variables, soil moisture content at depth 0 m was positively related to the success of mangrove regeneration. Higher elevation, slope, and air temperature have a negative relationship on mangrove regeneration. Greater distance from rivers or seasonal streams (i.e. wadis) also showed a negative relationship with mangrove regeneration. Precipitation had a positive effect on mangrove regeneration. There was also a strong positive correlation between mangrove regeneration and an interaction between minimum temperature and median precipitation. In case of the anthropogenic variables, population density showed a signifi-

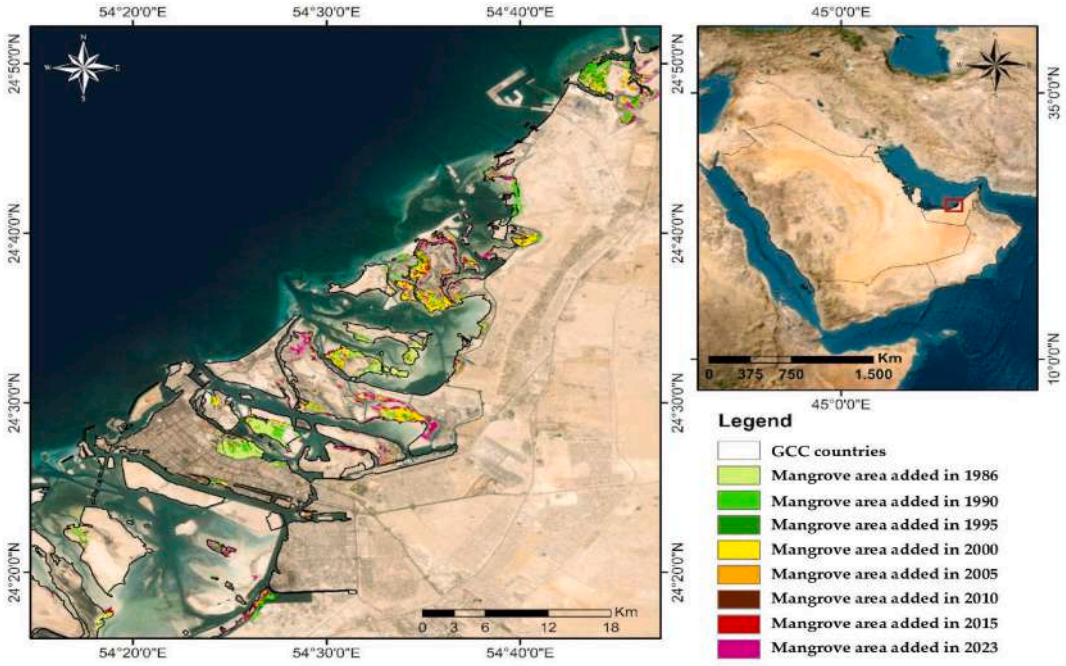

Fig. 6. Mangrove cover dynamics during the period 1986 to 2023 along the Abu Dhabi coastline, UAE.

cant negative relationship, while distance from roads had a significant positive relationship with mangrove regeneration. Interaction terms between distance from urban and agricultural areas also showed a weak but statistically significant correlation with mangrove regeneration success.

4. Discussion

In this study indices from multi-temporal Landsat time series imagery were used as input to the Random Forest machine learning algorithm to classify the mangrove cover across the GCC countries from 1986 to 2023. A secondary mangrove forest map was generated in order to identify mature mangrove stands with ages greater than 20 years. The location of these older stands was important to know as these allowed us to create a model to identify the key environmental and anthropogenic determinants, that were associated with their presence, and thereby influenced regeneration success (Utami et al., 2017; Sillanpää et al., 2017).

Our results show that only around 8.5% of secondary mangrove forests in the GCC region are older than 30 years, with mangroves younger than five years being the most abundant group at 41.3% (See Fig. 10). Saudi Arabia and Oman have the highest percentages of young mangroves, while relatively older secondary mangrove forests were most common in Bahrain, Qatar, and UAE. The present trends in overall mangrove area show that the UAE and Saudi Arabia have the highest mangrove area among the GCC countries, followed by Qatar, Oman, Bahrain, and Kuwait.

The mangrove cover (see Table 6) and mangrove loss and gain show the dynamics of mangrove presence in the GCC region. Saudi Arabia has shown an increase in mangrove cover from 1986 (2302 ha) to 2023 (6294 ha). This can be attributed to the plantation and nature-based solution initiatives that have been carried out since the 1990s, mainly by companies such as Saudi Aramco (Aramco, 2023; Li et al., 2019; National Geographic, 2023). To date, Saudi Aramco has planted over 24 million mangroves along the Arabian Gulf and Red Sea coastlines, out of which over 20 million have been planted since 2020. Moreover, in line with the Saudi Green Initiative and in collaboration with National Center for Vegetation Cover, Saudi Aramco plans to invest in planting 300 million mangroves in Saudi Arabia by 2035 (Saudi Aramco Sustainability Report, 2022), while Red Sea Global will plant 50 million mangroves by 2030 (Red Saudi Global Sustainability Report, 2022). The UAE is also regarded as one of the leading countries in the region in conserving and planting mangroves, with our results showing 22.1% growth in mangrove extent over the last two decades (2003–2023) representing a considerable gain of 1838 ha. These numbers are consistent with the UAE national strategy, that include mangrove initiatives such as the UAE target to plant 100 million mangroves by 2030 (Ahmar and Alfiky, 2023) in an effort to improve the country's carbon sequestration capacity (Friis and Killilea 2024). Qatar has also seen a gain of 27.4% in mangrove extent. In Oman a notable increase of 60% in mangrove area occurred from 2003 (118 ha) to 2023 (189 ha). This increase could be attributed to the national mangrove planting plan since 2002, which is an initiative in partnership with the government of Japan (UNEP, 2018). However, from our mapping methodology, it was not possible to ascertain to what extent the success of mangrove regeneration can be credited to afforestation programmes alone, since natural regeneration could also contribute to growth in areas adjacent to mature stands. Assessing the success of afforestation programmes to facilitate mangrove restoration in the GCC could be explored through future research.

Our mangrove cover results differ from the most widely used mangrove spatial database, Global Mangrove Watch (GMW) (Bunting et al., 2022). Most of the authors who had attempted to estimate the mangrove cover across countries in the GCC region us-

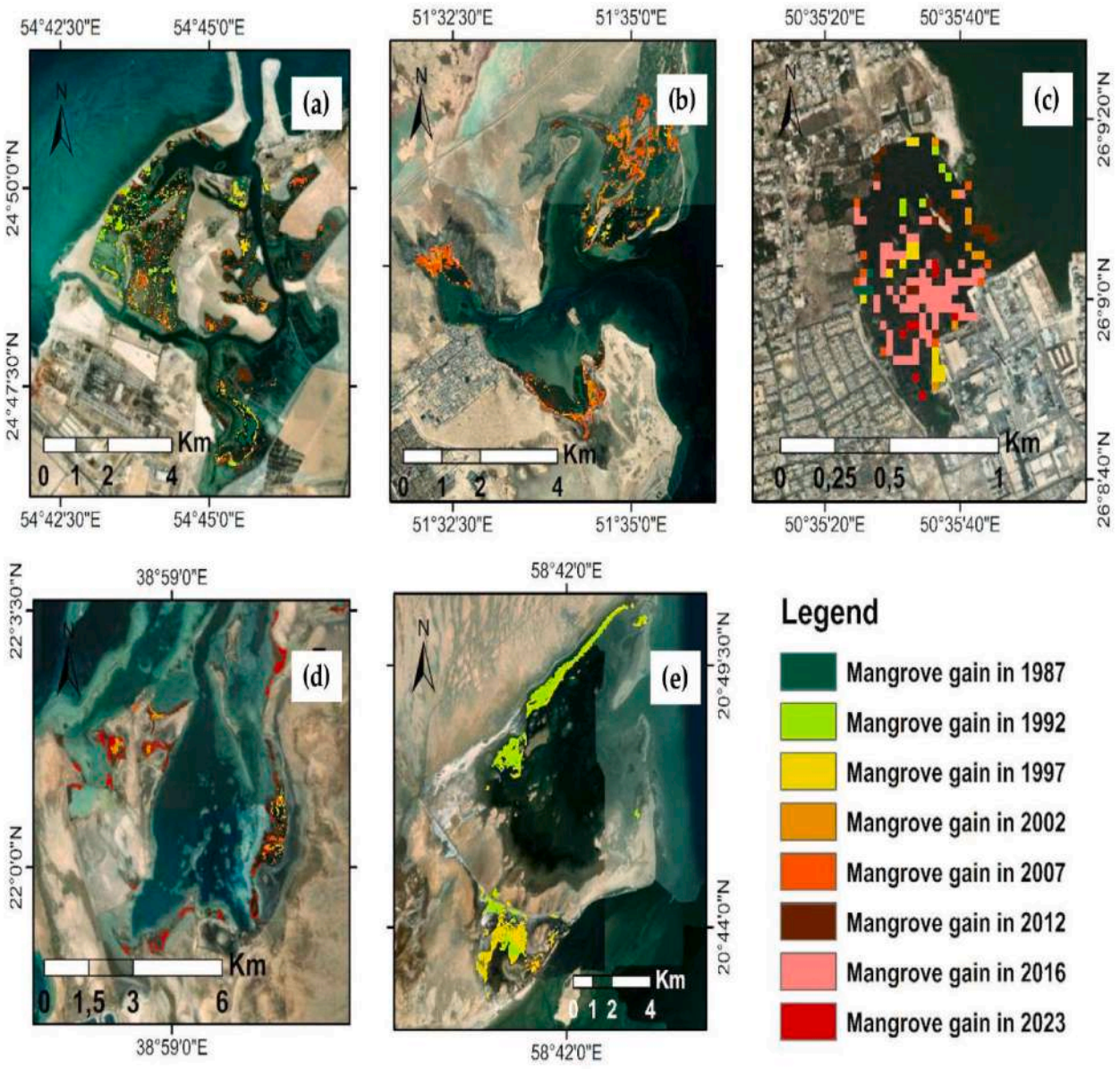

Fig. 7. Mangrove gain maps over the years 1987–2023 across key sites; Abu Dhabi in the UAE (a), Al Khawar and Adh Dhakhira in Qatar (b), Tubli Bay in Bahrain (c), coastline of Dhahaban in Saudi Arabia (d), and Al Wusta in Oman (e).

ing remote sensing data (13 studies), have not tested the accuracy for the classification technique used in their studies. In our recent work (Rondon et al., 2023), we noticed that the discrepancies in the mangrove cover results were attributed to the differences in mapping methods, classification techniques, the remotely sensed data, and spatial resolution (Guo et al., 2021; Rondon et al., 2023).

Our findings reveal the substantial contribution of specific environmental factors to mangrove growth success. Notably, higher availability of soil moisture, lower elevation and slope, higher precipitation, higher threshold of minimum temperature, proximity to freshwater sources like wadis, and anthropogenic factors such as lower population density and greater distance from urban centers, roads, and agricultural areas were most correlated to mangrove success (See Table 7). Factors like higher slope, elevation, proximity to rivers and population density have also been recorded as having negative effects on regeneration in mangrove forests of other locations such as in Vietnam and Iran (Pham and Yoshino 2016; Pir Bavaghar 2015). Positive correlations with factors such as soil moisture and the negative effect of distance to freshwater sources such as wadis align with studies that emphasize the influential role of freshwater access in enhancing mangrove growth rates (Erftemeijer et al., 2021; Santini et al., 2015). Knowledge of drivers of mangrove growth, such as the distribution of water and vegetation communities provides a means of characterizing the likelihood of successful growth of mangrove forests (Otero et al., 2020).

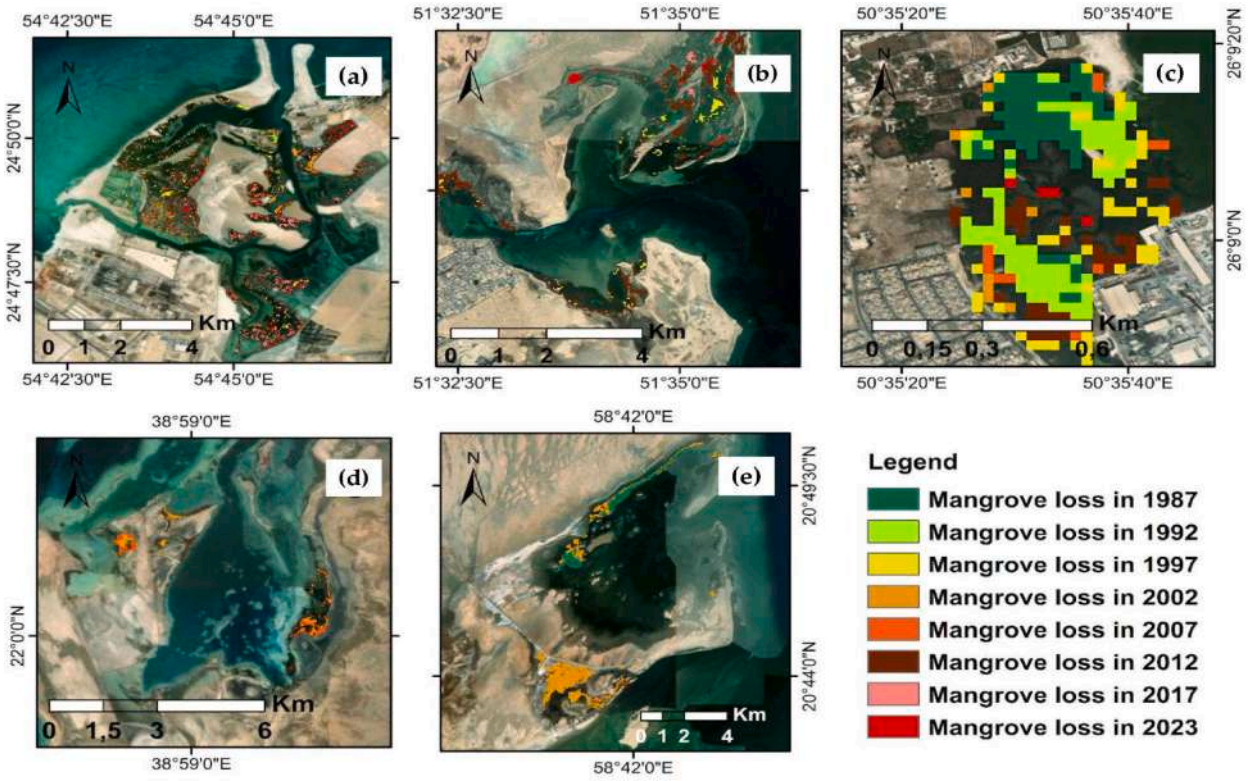

Fig. 8. Mangrove loss maps over the years 1987–2023 across key sites; Abu Dhabi in the UAE (a), Al Khawar and Adh Dhakhira in Qatar (b), Tubli Bay in Bahrain (c), coastline of Dhahaban in Saudi Arabia (d), and Al Wusta in Oman (e).

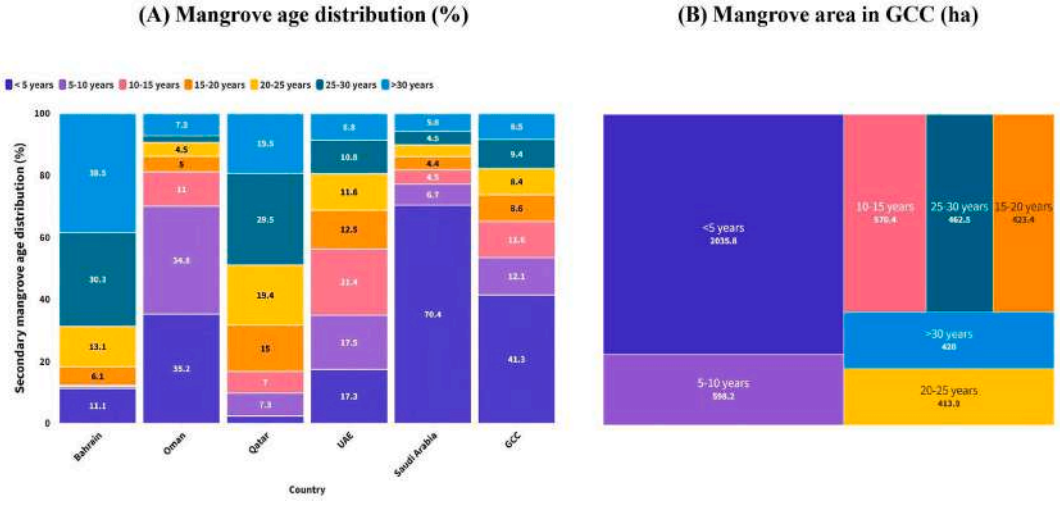

Fig. 9. Mangrove forest age in the GCC countries.

Our results in the GCC show how drivers such as soil moisture can positively contribute to successful mangrove regeneration. Restoration projects should focus on areas with higher soil moisture and access to freshwater. Targeting these areas can improve the likelihood of successful regeneration. Uptake of freshwater by the roots during rainfall supports mangrove growth and increased precipitation can increase mangrove ecosystem carbon stocks (Sanders et al., 2016; Steppe et al., 2018). Other factors in our study such as higher surface elevation, higher mean temperature and increased anthropogenic activities in the form of agriculture and urbanization have been found to be detrimental to mangrove regeneration. Mangroves in the GCC thrive in lower elevation sites on gentle slopes. Restoration initiatives should prioritize these areas to maximize the chances of mangrove establishment. Intertidal area has also been found as a key threshold to mangrove seedling establishment and successful regeneration. Higher surface elevation indicates that there is a shorter period of water exposure, thereby reducing seedling establishment (Oh et al., 2017). The strong relation

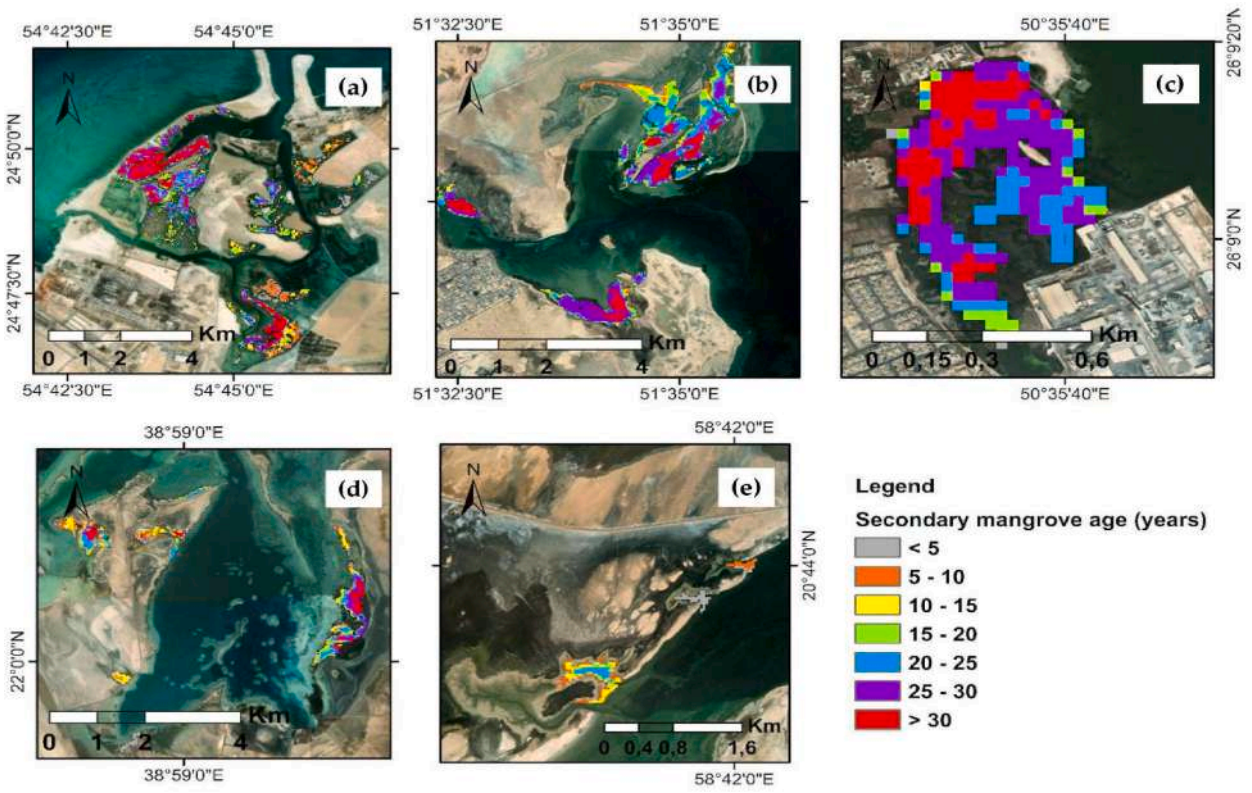

Fig. 10. Mangrove secondary age maps in 2023 across key sites; Abu Dhabi in the UAE (a), Al Khawar and Adh Dhakhira in Qatar (b), Western Akar in Bahrain (c), coastline of Dhahaban in Saudi Arabia (d), and Al Wusta in Oman (e).

Table 7
Stepwise logistic regression results for mangrove regeneration success in the GCC. In the 'Coefficient' column, the (∗) indicates p-values in ANOVA.

Category	Variable	Label	Standard Error	Coefficient	Odds ratio %
Environmental	Elevation	E1	0.19	−1.10 ([a])	−66.81%
	Slope	E2	0.03	−0.26([a])	−23.50%
	Minimum temperature	E3	0.8	0.9(NS)	−9.63%
	Mean temperature	E4	0.03	−0.245 ([a])	−21.87%
	Mean precipitation	E6	0.005	0.005(NS)	5.25%
	Maximum precipitation	E7	0.007	0.02([b])	2.19%
	Soil pH at depth 0 m	E8	0.02	0.04([c])	4.42%
	Soil moisture at depth 0 m	E10	0.006	0.13 ([a])	14.91%
	Distance from river	E12	0.004	−0.01 ([a])	−2.89%
	Minimum temperature x Mean precipitation	E3 x E6	0.33	4.08([a])	5845.37
Anthropogenic	Population density	A1	0.04	−0.14 ([c])	−13.24%
	Distance from agricultural areas	A2	0.002	0.002(NS)	−0.25%
	Distance from roads	A3	0.001	0.004([c])	0.42%
	Distance from urban areas	A4	0.007	0.006(NS)	0.74%
	Population density x Distance from agricultural areas	A1 x A2	0.001	0.0004(NS)	0.16%
	Population density x Distance from urban areas	A1 x A4	0.001	0.005([a])	0.55%
	Distance from agricultural areas x Distance from urban areas	A2 x A4	5.2×10^{-5}	0.0001([c])	0.01%
	Population density x Distance from agricultural areas x Distance from urban areas	A1 x A2 x A4	3.3×10^{-5}	−0.0001([b])	−0.01%

'NS' is not significant).
[a] < 0.001.
[b] < 0.01.
[c] < 0.05.

between the interaction of minimum temperature and precipitation to mangrove regeneration was attributable to the significant increase in mangrove regeneration in areas with a higher threshold of minimum temperature and higher availability of freshwater. This could be attributed to the affinity of mangroves to temperatures above 20 °C and their mortality by frost incidents at higher latitudes (Ellison, 2021).

Increasing distances from urban areas had a significant positive impact on mangroves regeneration. This aligns with the findings of Arshad et al. (2020), showing that the main anthropogenic processes contributing to coastal wetlands and mangrove forest loss are associated with land reclamation, and coastal development is considered to be the primary anthropogenic threat to coastal ecosystems in the Arabian Gulf. This could be attributed to the rapid urbanization in the GCC, where coastal development is widespread around growing urban centers and often heavily impacts coastal ecosystems such as mangrove forests (Burt 2014; Sale et al., 2011). To mitigate the negative impacts of urbanization, buffer zones can be implemented around urban areas to protect existing mangrove forests. Policies should be enforced to limit coastal development in critical mangrove habitats. In the Tubli Bay area of Bahrain, mangrove cover witnessed a decline over the past half-century, directly attributed to reclamation activities (Aljenaid et al., 2022). In the Dammam Metropolitan Area in the eastern coast of Saudi Arabia, coastal reclamation has increased due to urbanization strategies, such as commercial, industrial and leisure activities, impacting mangrove forest and other marine ecosystems negatively (AlQahtany et al., 2022). In the area of Tarut Bay (Saudi Arabia) population pressures mediated by urban encroachment and land reclamation led to major losses (55%) (Almahasheer, 2018). The UAE also has experienced the consequences of the intense urban development and land reclamation in coastal zones since the early 2000, negatively affecting mangrove cover in some areas (Friis and Killilea, 2024), although the dredging of channels into lagoonal areas has also been suggested to reduce salinity and foster enhanced growth (Burt et al., 2021). The degradation of mangroves trees in the Red Sea region has also been observed for several anthropogenic activities such as grazing of camels, shrimp farming and construction activities altering water level (Aljahdali et al., 2021). Collaborative efforts can amplify the impact of restoration projects and ensure sustainable management practices by the various stakeholders.

Some of the main limitations of our studies are related to using the Landsat series as the only spatial data source and using only a single composite image for the classification each year. Obtaining other high-resolution satellite images for the entire time period was not possible due to cost, availability and time constraints. Vegetation indices such as the Submerged Mangrove Recognition Index (SMRI) assists an understanding of mangroves in submerged conditions using the spectral differences of two images from high and low tides (Xia et al., 2018, 2020). Using SMRI Li et al. (2019) demonstrated good accuracy in identifying submerged mangroves in Saudi Arabia, but this index could not be used in our study. The lack of data consistency of Landsat 5 in the coastal areas of the GCC region, especially in the years between 2001 and 2012, and the data loss due to the scan line corrector (SLC)-off imagery in mangroves as a result of SLC failure in Landsat 7 are well recognized (Hossain et al., 2015). Moreover, the collection of spatiotemporally stable pixels for training data may pose a bias towards older and established forests, overlooking the younger mangroves. This could have led to a few 1-year outliers, such as in 1992 in Saudi Arabia, 1994 in the UAE, 1990 and 1995 in Oman and 2001 in Qatar. These outliers can potentially influence the total mangrove area of GCC for those years. Using our mapping methodology, it was also not possible to differentiate natural regeneration from artificial regeneration. There were also some limitations related to the anthropogenic variables. Raster layers of factors such as distance from agricultural and urban areas were created by applying a median reducer on LULC maps spanning multiple years. Considering the rapid change and urbanization in the coastal GCC recently, we acknowledge this might be a potential drawback in our methodology. Certain potential drivers for mangrove regeneration such as seawater salinity levels and temperature could not be evaluated using logistic regression because this data was unavailable in many areas in the coastal GCC. Some remote-sensing based predictors for the logistic regression like CHIRPS and MODIS LST had coarse spatial resolution, which reduces the model sensitivity for localized applications.

Considering that mangrove forests form a minor land cover class in the GCC region, it is important to develop new applications of remote sensing that can make use of this technology on a smaller scale for studying these ecosystems more effectively (Rondon et al., 2023). Data fusion of multispectral images with other sensors such as SAR has also shown potential in studying mangroves in other parts of the globe (Souza-Filho et al., 2009), which can be applied in the GCC. SAR can be useful to study the vertical structure of the forest based on interferometric configurations. We also recommend better availability of openly accessible remotely sensed environmental data at higher spatial resolution for increasing the accuracy in modeling the drivers of mangrove regeneration. UAVs can be an effective solution to identify areas where rehabilitation should be conducted (Darmawan et al., 2020). They have the potential to save upwards of USD 30,000 per ha as compared to on-ground measurements (Navarro et al., 2020). Moreover, they can be used not only in monitoring, but also for actively promoting rapid afforestation. UAV-supported seed sowing is a safe, cost-effective, fast and environmentally friendly method of establishment (Mohan et al., 2021). We recommend using additional factors, including the presence and effectiveness of protected areas to study drivers influencing mangrove regeneration. Finally, in terms of cost for instance, the C-band Sentinel-1 data from the European Space Agency (ESA) or the data of the future P-band BIOMASS mission also from ESA or the L&S-band NiSAR mission from the US-Indian NASA-ISRO are fully accessible which is consistent with the open data policies adopted by these space agencies.

5. Conclusion

In this study, we identified the drivers for successful mangrove growth in the GCC region by using secondary mangrove forests as a baseline to age mangrove stands. The study determined the mangrove area throughout the GCC using Random Forest classifiers that used indices derived from Landsat data. The predictions on the validation dataset had outstanding performance for most country/year combinations as highlighted by F1-scores that mostly exceeded 0.9. The spatial distribution of older mangroves provides insights into the prevailing conditions, both environmental and anthropogenic, that have influenced mangrove community survival over time. Our results show that the main drivers that contribute to mangrove establishment success are lower elevation, lower slope, greater proximity to freshwater sources, and available soil moisture at 30 cm rootable depth (environmental) and lower population density and greater distance from urban areas (anthropogenic). Our approach offers support for decision-makers in selecting optimal areas for new planting initiatives. By taking into account the areas with similar environmental and anthropogenic factors, our methodology

aims to increase the seedling and propagule survival rate. Additionally, determining mangrove age, an important outcome of our study, holds significance for governments and conservation stakeholders. This information is crucial for making informed decisions, promoting sustainable management practices, and ensuring the effective conservation of these vital ecosystems. The main limitations of our study were the use of one spatial data source, lack of data consistency, especially in the earlier years, and using only openly accessible remote sensing data for studying the potential driving factors of mangrove regeneration success. Future studies are encouraged to address the limitations we faced in our work, with the aim of extending the proposed approach for enhancing mangrove conservation, ecotourism initiatives, community engagement and carbon market programs both regionally and globally (Karpowicz et al., 2024; Moussa et al., 2024; Dutta Roy et al., 2024; Blanton et al., 2024).

Ethical statement

All ethical practices have been followed in relation to the development, writing, and publication of the article.

CRediT authorship contribution statement

Midhun Mohan: Writing – review & editing, Writing – original draft, Validation, Supervision, Project administration, Methodology, Investigation, Data curation, Conceptualization. **Abhilash Dutta Roy:** Writing – review & editing, Writing – original draft, Supervision, Project administration, Methodology, Investigation, Formal analysis, Conceptualization. **Jorge F. Montenegro:** Writing – original draft, Supervision, Project administration. **Michael S. Watt:** Writing – review & editing, Methodology, Conceptualization. **John A. Burt:** Writing – review & editing. **Aurelie Shapiro:** Writing – review & editing. **Dhouha Ouerfelli:** Writing – review & editing, Writing – original draft, Visualization, Validation, Methodology, Investigation, Formal analysis. **Redeat Daniel:** Writing – original draft, Visualization, Methodology, Investigation, Formal analysis. **Sergio de-Miguel:** Writing – review & editing, Supervision. **Tarig Ali:** Writing – review & editing. **Macarena Ortega Pardo:** Writing – review & editing. **Mario Al Sayah:** Writing – review & editing. **Valliyil Mohammed Aboobacker:** Writing – review & editing. **Naji El Beyrouthy:** Writing – review & editing. **Ruth Reef:** Writing – review & editing. **Esmaeel Adrah:** Writing – review & editing, Visualization, Methodology, Investigation. **Reem AlMealla:** Writing – review & editing. **Pavithra S. Pitumpe Arachchige:** Writing – review & editing. **Pandi Selvam:** Writing – review & editing, Raluca Diaconu, Writing – review & editing. **Wan Shafrina Wan Mohd Jaafar:** Writing – review & editing. **Lara Sujud:** Writing – review & editing. **Jenan Bahzad:** Writing – review & editing. **Isuru Alawatte:** Writing – review & editing. **Sohaib Hussein:** Writing – review & editing. **Carlos López-Martínez:** Writing – review & editing. **Frida Sidik:** Writing – review & editing. **Manickam Nithyanandan:** Writing – review & editing. **Meshal Abdullah:** Writing – review & editing, Writing – review & editing. **Ammar Abulibdeh:** Writing – review & editing. **Adrián Cardil:** Writing – review & editing, Willie Doaemo, Writing – review & editing. **Jeffrey Q. Chambers:** Writing – review & editing.

Declaration of competing interest

The authors declare the following financial interests/personal relationships which may be considered as potential competing interests: Midhun Mohan reports a relationship with Ecoresolve that includes: employment. Abhilash Dutta Roy reports a relationship with Ecoresolve that includes: employment. Jorge F. Montenegro reports a relationship with Ecoresolve that includes: employment. Dhouha Ouerfelli reports a relationship with Ecoresolve that includes: employment. Redeat Daniel reports a relationship with Ecoresolve that includes: employment. Pavithra S. Pitumpe Arachchige reports a relationship with Ecoresolve that includes: employment. If there are other authors, they declare that they have no known competing financial interests or personal relationships that could have appeared to influence the work reported in this paper.

Acknowledgments

We are thankful to the following authors who contributed to the review of the article: Lara Moussa, Raluca Diaconu, Gilberto Pastorello, Basil Ewane, Willie Doaemo and Humood Abdulla Naser. We would like to thank UC Berkeley for supporting the open access publication of this article. The summer grant from UC Berkeley Geography Department (for Dr. Midhun Mohan) also partially supported this research.

Data availability

Data will be made available on request.

References

Ahmar, A., Alfiky, A., 2023. UAE Looks to Salty, Muddy Mangroves in Climate Change Fight. June 12. Reuters. https://www.reuters.com/world/middle-east/uae-looks-salty-muddy-mangroves-climate-change-fight-2023-06-12/.

Al-Ansari, E.M.A.S., Husrevoglu, Y.S., Yigiterhan, O., et al., 2022. Seasonal variability of hydrography off the east coast of Qatar, central Arabian Gulf. Arabian J. Geosci. 15, 1659. https://doi.org/10.1007/s12517-022-10927-4.

Aljahdali, M.O., Munawar, S., Khan, W.R., 2021. Monitoring mangrove forest degradation and regeneration: landsat time series analysis of moisture and vegetation indices at rabigh lagoon, Red Sea. Forests 12 (1). https://doi.org/10.3390/f12010052. Article 1.

Aljenaid, S., Abido, M., Redha, G.K., AlKhuzaei, M., Marsan, Y., Khamis, A.Q., Naser, H., AlRumaidh, M., Alsabbagh, M., 2022. Assessing the spatiotemporal changes, associated carbon stock, and potential emissions of mangroves in Bahrain using GIS and remote sensing data. Reg. Stud. Marine Sci. 52, 102282. https://doi.org/10.1016/j.rsma.2022.102282.

Al-Dubai, T.A., Abu-Zied, R.H., Basaham, A.S., 2017. Present environmental status of Al-Kharrar Lagoon, central of the eastern Red Sea coast, Saudi Arabia. Arabian J.

Geosci. 10 (14), 305. https://doi.org/10.1007/s12517-017-3083-0.
Almahasheer, H., 2018. Spatial coverage of mangrove communities in the Arabian Gulf. Environ. Monit. Assess. 190 (2), 85. https://doi.org/10.1007/s10661-018-6472-2.
Almahasheer, H., 2019. High levels of heavy metals in Western Arabian Gulf mangrove soils. Mol. Biol. Rep. 46 (2), 1585–1592. https://doi.org/10.1007/s11033-019-04603-2.
AlQahtany, A.M., Dano, U.L., Elhadi Abdalla, E.M., Mohammed, W.E.M., Abubakar, I.R., Al-Gehlani, W.A.G., Akbar, N., Alshammari, M.S., 2022. Land reclamation in a coastal metropolis of Saudi Arabia: environmental sustainability implications. Water 14 (16). https://doi.org/10.3390/w14162546. Article 16.
Alsumaiti, T.S., 2017. Mapping changes in mangrove forests and the future impacts of sea level rise in Abu Dhabi, United Arab Emirates. Int. J. Basic Appl. Sci. 7 (1), 57–61.
Alsumaiti, T., Shahid, S., 2019. Mangroves among most carbon-rich ecosystem living in hostile saline rich environment and mitigating climate change -A case of Abu Dhabi. J. Agric. Crop Res. 7, 1–8.
Aramco, 2023. Mangrove initiatives. https://www.aramco.com/en/sustainability/minimizing-environmental-impact/biodiversity-and-land-use/promoting-biodiversity/mangrove-initiatives.
Arshad, M., Eid, E.M., Hasan, M., 2020. Mangrove health along the hyper-arid southern Red Sea coast of Saudi Arabia. Environ. Monit. Assess. 192 (3), 189. https://doi.org/10.1007/s10661-020-8140-6.
Assaf, H., Idwan, S., Jallad, A.H., Ammari, M.Z.J., Chaar, A.A., Kouja, M., 2022. Public values regarding an urban mangrove wetland in the United Arab Emirates. J. Environ. Eng. Landsc. Manag. 30 (1). https://doi.org/10.3846/jeelm.2022.16333. Article 1.
Bashour, I.I., Al-Mashhady, A.S., Devi Prasad, J., Miller, T., Mazroa, M., 1983. Morphology and composition of some soils under cultivation in Saudi Arabia. Geoderma 29 (4), 327–340.
Barbier, E., Hacker, S., Kennedy, C., 2011. The value of estuarine and coastal ecosystem services. Ecological Ldots 81, 169–193.
Blanco-Sacristán, J., Johansen, K., Duarte, C.M., Daffonchio, D., Hoteit, I., McCabe, M.F., 2022. Mangrove distribution and afforestation potential in the Red Sea. Sci. Total Environ. 843, 157098. https://doi.org/10.1016/j.scitotenv.2022.157098.
Blanton, A., Ewane, E.B., McTavish, F., Watt, M.S., Rogers, K., Daneil, R., Mohan, M., 2024. Ecotourism and mangrove conservation in Southeast Asia: Current trends and perspectives. J. Environ. Manag. 365, 121529.
Breiman, L., 2001. Random forests. January 1. Mach. Learn. https://doi.org/10.1023/a:1010933404324.
Buchhorn, M., Lesiv, M., Tsendbazar, N.-E., Herold, M., Bertels, L., Smets, B., 2020. Copernicus global land cover layers-collection 2. Rem. Sens. 108, 1044. https://doi.org/10.3390/rs12061044. 12Volume.
Bunting, P., Rosenqvist, A., Lucas, R.M., Rebelo, L.M., Hilarides, L., Thomas, N., et al., 2018. The global mangrove watch—a new 2010 global baseline of mangrove extent. Rem. Sens. 10 (10), 1669. https://doi.org/10.3390/rs10101669.
Bunting, P., Rosenqvist, A., Hilarides, L., Lucas, R.M., Thomas, N., Tadono, T., Worthington, T.A., Spalding, M., Murray, N.J., Rebelo, L.-M., 2022. Global mangrove extent change 1996–2020: global mangrove watch version 3.0. Rem. Sens. 14 (15). https://doi.org/10.3390/rs14153657. Article 15.
Burt, J., 2014. The environmental costs of coastal urbanization in the Arabian Gulf. City: analysis of urban trends, culture, theory. Policy & Action 18 (6), 760–770. https://doi.org/10.1080/13604813.2014.962889.
Burt, J.A., Bartholomew, A., 2019. Towards more sustainable coastal development in the Arabian Gulf: opportunities for ecological engineering in an urbanized seascape. Mar. Pollut. Bull. 142, 93–102. https://doi.org/10.1016/j.marpolbul.2019.03.024.
Burt, J., Killilea, M., Rademacher, A., 2021. Unexpected nature? Proliferating mangroves on the coast of Abu Dhabi. In: Durr, E., Keller, R. (Eds.), Urban Environments as Spaces of Living in Transformation: Position Papers Collection. Urban Environments Initiative, Rachel Carson Center, pp. 44–47. https://urbanenv.org/wp-content/uploads/2021/01/PDF-Collection.pdf#page=45.
Burt, J.A., Paparella, F., 2023. The marine environment of the Emirates. In: Burt, J.A. (Ed.), A Natural History of the Emirates. Springer Nature, pp. 95–117. https://doi.org/10.1007/978-3-031-37397-8_4.
Carvalho, S., Kürten, B., Krokos, G., Hoteit, I., Ellis, J., 2019. The Red Sea. In: Sheppard, C. (Ed.), World Seas: an Environmental Evaluation, vol. II. Elsevier, pp. 49–74. https://doi.org/10.1016/b978-0-08-100853-9.00004-x.
Chithambaran, S., 2019. Restoration of mangrove vegetation at Red Sea coast, Saudi Arabia. Indian J. Geo Marine Sci. 48 (11), 1755–1760.
Climate Watch, 2022. Climate watch. https://www.climatewatchdata.org/.
Clüsener-Godt, M., Cárdenas Tomažič, M.R., 2016. 8 - the importance of mangrove ecosystems for nature protection and food productivity: actions of UNESCO's man and the biosphere programme. In: Khan, M.A., Ozturk, M., Gul, B., Ahmed, M.Z. (Eds.), Halophytes for Food Security in Dry Lands. Academic Press, pp. 125–140. https://doi.org/10.1016/B978-0-12-801854-5.00008-X.
Cissell, J.R., Canty, S.W., Steinberg, M.K., Simpson, L.T., 2021. Mapping national mangrove cover for Belize using Google Earth Engine and Sentinel-2 imagery. Appl. Sci. 11 (9), 4258. https://doi.org/10.3390/app11094258.
Cougo, M.F., Souza-Filho, P.W.M., Silva, A.Q., Fernandes, M.E.B., Santos, J. R. dos, Abreu, M.R.S., Nascimento, W.R., Simard, M., 2015. Radarsat-2 backscattering for the modeling of biophysical parameters of regenerating mangrove forests. Rem. Sens. 7 (12). https://doi.org/10.3390/rs71215873. Article 12.
Darmawan, A., Saputra, D.K., Asadi, M.A., Karang, I.W.G.A., 2020. UAV application for site suitability mangrove replantation program, case study in Pasuruan and Probolinggo, East Java. In: E3S Web of Conferences, vol. 153. EDP Sciences, 01009.
Diniz, C.G., Cortinhas, L., Nerino, G., Rodrigues, J., Sadeck, L.W.R., Adami, M., Souza-Filho, P.W.M., 2019. Brazilian mangrove status: three decades of satellite data analysis. April 4. Rem. Sens. https://doi.org/10.3390/rs11070808.
Donato, D.C., Kauffman, J.B., Murdiyarso, D., Kurnianto, S., Stidham, M., Kanninen, M., 2011. Mangroves among the most carbon-rich forests in the tropics. Nat. Geosci. 4 (5). https://doi.org/10.1038/ngeo1123. Article 5.
Dutta Roy, A., Arachchige, P.S.P., Watt, M.S., Kale, A., Davies, M., Heng, J.E., Mohan, M., 2024. Remote sensing-based mangrove blue carbon assessment in the Asia-Pacific: A systematic review. Sci. Total Environ. 938, 173270. . Chicago.
Ellison, J.C., 2021. Factors influencing mangrove ecosystems. In: Rastogi, R.P., Phulwaria, M., Gupta, D.K. (Eds.), Mangroves: Ecology, Biodiversity and Management. Springer, Singapore, pp. 97–115. https://doi.org/10.1007/978-981-16-2494-0_4.
Elmahdy, S., Ali, T., Mohamed, M., 2020a. Flash flood susceptibility modeling and magnitude index using machine learning and geohydrological models: a modified hybrid approach. Rem. Sens. 12 (17), Scopus. https://doi.org/10.3390/RS12172695.
Elmahdy, S.I., Ali, T.A., Mohamed, M.M., Howari, F.M., Abouleish, M., Simonet, D., 2020b. Spatiotemporal mapping and monitoring of mangrove forests changes from 1990 to 2019 in the northern Emirates, UAE using random forest, kernel logistic regression and naive bayes tree models. Front. Environ. Sci. 8. https://www.frontiersin.org/articles/10.3389/fenvs.2020.00102.
Elobaid, E.A., Al-Ansari, E.M.A.S., Yigiterhan, O., Aboobacker, V.M., Vethamony, P., 2022. Spatial variability of summer hydrography in the central Arabian Gulf. Oceanologia 64, 75–87.
Erftemeijer, P.L.A., Cambridge, M.L., Price, B.A., Ito, S., Yamamoto, H., Agastian, T., Burt, J.A., 2021. Enhancing growth of mangrove seedlings in the environmentally extreme Arabian Gulf using treated sewage sludge. Mar. Pollut. Bull. 170, 112595. https://doi.org/10.1016/j.marpolbul.2021.112595.
Fatoyinbo, T.E., Simard, M., Washington-Allen, R.A., Shugart, H.H., 2008. Landscape-scale extent, height, biomass, and carbon estimation of Mozambique's mangrove forests with Landsat ETM+ and Shuttle Radar Topography Mission elevation data. J. Geophys. Res.: Biogeosciences 113 (G2). https://doi.org/10.1029/2007JG000551.
Firmin, R., 1968. Forestry trials with high saline restoration of or sea water in Kuwait. In: Boyko, H. (Ed.), Saline Irrigation for Agriculture and Forestry. Dr W Junk NV Publishers, The Hague, pp. 107–132.
Friis, G., Burt, J.A., 2020. Evolution of mangrove research in an extreme environment: historical trends and future opportunities in Arabia. Ocean Coast Manag. 195, 105288. https://doi.org/10.1016/j.ocecoaman.2020.105288.
Friis, G., Killilea, M.E., 2024. Mangrove ecosystems of the United Arab Emirates. In: Burt, J.A. (Ed.), A Natural History of the Emirates. Springer, Nature Switzerland, pp. 217–240. https://doi.org/10.1007/978-3-031-37397-8_7.
Funk, C., Peterson, P., Landsfeld, M., et al., 2015. The climate hazards infrared precipitation with stations—a new environmental record for monitoring extremes. Sci.

Data 2, 150066. https://doi.org/10.1038/sdata.2015.66.
Getzner, M., Islam, M.S., 2020. Ecosystem services of mangrove forests: results of a meta-analysis of economic values. Int. J. Environ. Res. Publ. Health 17 (16). https://doi.org/10.3390/ijerph17165830. Article 16.
Gorman, D., Vanderklift, M., Lafratta, A., 2022. Quantitative analysis of methodological and environmental influences on survival of planted mangroves in restoration and afforestation. Forests 13, 404. https://doi.org/10.3390/f13030404.
Gilani, H., Naz, H.I., Arshad, M., Nazim, K., Akram, U., Abrar, A., Asif, M., 2021. Evaluating mangrove conservation and sustainability through spatiotemporal (1990–2020) mangrove cover change analysis in Pakistan. Estuar. Coast Shelf Sci. 249, 107128. https://doi.org/10.1016/j.ecss.2020.107128.
Gorelick, N., Hancher, M., Dixon, M., Ilyushchenko, S., Thau, D., Moore, R., 2017. Google Earth engine: planetary-scale geospatial analysis for everyone. Rem. Sens. Environ. 202, 18–27.
Gupta, K., Mukhopadhyay, A., Giri, S., Chanda, A., Majumdar, S.D., Samanta, S., Mitra, D., Samal, R.N., Pattnaik, A.K., Hazra, S., 2018. An index for discrimination of mangroves from non-mangroves using LANDSAT 8 OLI imagery. MethodsX (5), 1129–1139. https://doi.org/10.1016/j.mex.2018.09.011.
Guo, Y., Liao, J., Shen, G., 2021. Mapping large-scale mangroves along the maritime silk road from 1990 to 2015 using a novel deep learning model and landsat data. Rem. Sens. 13 (2). https://doi.org/10.3390/rs13020245. Article 2.
Habibullah, M., Haji Din, B., Tan, S., Zahid, H., 2022. Impact of climate change on biodiversity loss: global evidence. Environ. Sci. Pollut. Control Ser. 29. https://doi.org/10.1007/s11356-021-15702-8.
Hegazy, A.K., 1998. Perspectives on survival, phenology, litter fall and decomposition, and caloric content of Avicennia marinain the Arabian Gulf region. J. Arid Environ. 40 (4), 417–429. https://doi.org/10.1006/jare.1998.0457.
Hengl, T., 2018. Soil pH in H2O at 6 standard depths (0, 10, 30, 60, 100 and 200 cm) at 250 m resolution (Version v02). Zenodo. https://doi.org/10.5281/zenodo.1475459. [Data set].
Hengl, T., Gupta, S., 2019. Soil water content (volumetric %) for 33kPa and 1500kPa suctions predicted at 6 standard depths (0, 10, 30, 60, 100 and 200 cm) at 250 m resolution (Version v01). Zenodo. https://doi.org/10.5281/zenodo.2629589. [Data set].
Hereher, M., Al-Awadhi, T., 2019. Remote sensing of coastal ecosystems using spectral indices. 5. https://doi.org/10.1145/3387168.3387174.
Hickey, S.M., Radford, B., 2022. Turning the tide on mapping marginal mangroves with multi-dimensional space–time remote sensing. Rem. Sens. 14 (14). https://doi.org/10.3390/rs14143365. Article 14.
Hossain, M.S., Bujang, J.S., Zakaria, M.H., Hashim, M., 2015. Assessment of the impact of landsat 7 scan line corrector data gaps on sungai pulai estuary seagrass mapping. Appl. Geo. 7, 189–202.
Ismail, E., Hussein, H., 2022. TAQA, AQDAR, Blue Forest partner on UAE's largest employee-led tree planting initiative to mark UAE's 50th. February 20. Wam. https://wam.ae/en/details/1395303022597.
Jamaluddin, I., Chen, Y.N., Ridha, S.M., Mahyatar, P., Ayudyanti, A.G., 2022. Two decades mangroves loss monitoring using random forest and landsat data in east luwu, Indonesia (2000–2020). July 22. Geom. 2 (3), 282–296. https://doi.org/10.3390/geomatics2030016.
Jarvis, A., Reuter, H.I., Nelson, A., Guevara, E., 2008. Hole-filled SRTM for the globe version 4, available from the CGIAR-CSI SRTM 90m database. https://srtm.csi.cgiar.org.
Karpowicz, D.A., Mohan, M., Watt, M.S., Montenegro, J.F., King, S.A., Selvam, P.P., Ewane, E.B., 2024. Mangrove-based carbon market projects: 15 considerations for engaging and supporting local communities. Diversity 16 (9), 574.
Khader, H., 2023. Mangroves in Qatar: perspectives [EcoMENA]. March 23. https://www.ecomena.org/mangroves-in-qatar/.
Krauss, K., Lovelock, C., Chen, L., Berger, U., Ball, M., Reef, R., Peters, R., Bowen, H., Vovides, A., Ward, E., Wimmler, M.-C., Carr, J., Bunting, P., Duberstein, J., 2022. Mangroves provide blue carbon ecological value at a low freshwater cost. Sci. Rep. 12. https://doi.org/10.1038/s41598-022-21514-8.
Leandro, P., Knuteson, S.L., Bartholomew, A., 2022. The vegetation of the United Arab Emirates Gulf coast: description and analysis. J. Coast Res. 38 (5), 951–967. https://doi.org/10.2112/JCOASTRES-D-21-00162.1.
Li, W., El-Askary, H., Qurban, M.A., Li, J., ManiKandan, K.P., Piechota, T., 2019. Using multi-indices approach to quantify mangrove changes over the Western Arabian Gulf along Saudi Arabia coast. Ecol. Indicat. 102, 734–745. https://doi.org/10.1016/j.ecolind.2019.03.047.
Loughland, R., Butt, S.J., Nithyanandan, M., 2020. Establishment of mangrove ecosystems on man-made islands in Kuwait: sustainable outcomes in a challenging and changing environment. Aquat. Bot. 167, 103273. https://doi.org/10.1016/j.aquabot.2020.103273.
Lutz, S., Massuanganhe, E., Nicolau, D.K., Bandeira, S.O., Adams, J.B., 2011. Blue carbon - first level exploration of natural coastal carbon in the arabian peninsula, with special focus on the UAE and Abu Dhabi: a rapid feasibility study 2011. UNEP/GRID-ArendaMacamo, C. C. F. Mangrove's response to cyclone Eline (2000): What is happening 14 years later. Aquatic Botany 134, 10–17. https://doi.org/10.1016/j.aquabot.2016.05.004. 2016.
Mafi-Gholami, D., Jaafari, A., Zenner, E.K., Nouri Kamari, A., Tien Bui, D., 2020. Spatial modeling of exposure of mangrove ecosystems to multiple environmental hazards. Sci. Total Environ. 740, 140167. https://doi.org/10.1016/j.scitotenv.2020.140167.
Mafi-Gholami, D., Pirasteh, S., Ellison, J.C., Jaafari, A., 2021. Fuzzy-based vulnerability assessment of coupled social-ecological systems to multiple environmental hazards and climate change. J. Environ. Manag. 299, 113573. https://doi.org/10.1016/j.jenvman.2021.113573.
Mahamunkar, G.S., Kiwelekar, A.W., Netak, L.D., 2022. Mapping and change detection of mangroves using remote sensing and Google Earth engine: a case study. In: Tuba, M., Akashe, S., Joshi, A. (Eds.), ICT Systems and Sustainability. Springer Nature, pp. 187–195. https://doi.org/10.1007/978-981-16-5987-4_20.
Mateos-Molina, D., Ben Lamine, E., Antonopoulou, M., Burt, J.A., Das, H.S., Javed, S., Judas, J., Khan, S.B., Muzaffar, S.B., Pilcher, N., Rodriguez-Zarate, C.J., Taylor, O.J.S., Giakoumi, S., 2021. Synthesis and evaluation of coastal and marine biodiversity spatial information in the United Arab Emirates for ecosystem-based management. Mar. Pollut. Bull. 167, 112319. https://doi.org/10.1016/j.marpolbul.2021.112319.
Milani, A.S., 2018. Mangrove forests of the Persian Gulf and the Gulf of Oman. In: Makowski, C., Finkl, C.W. (Eds.), Threats to Mangrove Forests: Hazards, Vulnerability, and Management. Springer International Publishing, pp. 53–75. https://doi.org/10.1007/978-3-319-73016-5_3.
Mohan, M., Richardson, G., Gopan, G., Aghai, M.M., Bajaj, S., Galgamuwa, G.P., et al., 2021. UAV-supported forest regeneration: current trends, challenges and implications. Rem. Sens. 13 (13), 2596.
Mohanty, S., Mustak, Sk, Singh, D., Van Hoang, T., Mondal, M., Wang, C.-T., 2023. Vulnerability and risk assessment mapping of Bhitarkanika national park, Odisha, India using machine-based embedded decision support system. Front. Environ. Sci. 11. https://www.frontiersin.org/articles/10.3389/fenvs.2023.1176547.
Morgan, J., 2023. UAE endorses global $4 billion investment by 2030 to conserve mangroves. September 21. Natl. NOW Times. https://www.thenationalnews.com/uae/2023/09/21/uae-endorses-global-4-billion-investment-by-2030-to-conserve-mangroves/.
Moussa, L.G., Mohan, M., Burmeister, N., King, S.A., Burt, J.A., Rog, S.M., Ewane, E.B., 2024. Mangrove ecotourism along the coasts of the Gulf Cooperation Council countries: A systematic review. Land 13 (9), 1351. https://doi.org/10.3390/land13091351.
Nardin, T., Piasentier, E., Barnaba, C., Larcher, R., 2016. Targeted and untargeted profiling of alkaloids in herbal extracts using online solid-phase extraction and high resolution mass spectrometry (Q-Orbitrap). J. Mass Spectrom. 51. https://doi.org/10.1002/jms.3838.
National Geographic, 2023. The mangroves solution. https://www.nationalgeographic.com/protecting-a-natural-kingdom/the-mangroves-solution/.
Navarro, A., Young, M., Allan, B., Carnell, P., Macreadie, P., Ierodiaconou, D., 2020. The application of Unmanned Aerial Vehicles (UAVs) to estimate above-ground biomass of mangrove ecosystems. Rem. Sens. Environ. 242, 111747.
Nguyen, T.T.H., 2019. Drivers of forest change in Hoa Binh, Vietnam in the context of integration and globalization. Singapore J. Trop. Geogr. 40 (3), 452–475. https://doi.org/10.1111/sjtg.12289.
Oh, R.R.Y., Friess, D.A., Brown, B.M., 2017. The role of surface elevation in the rehabilitation of abandoned aquaculture ponds to mangrove forests, Sulawesi, Indonesia. Ecol. Eng. 100, 325–334.
Oliver, L., Hahn, K., Barrows, R., Jarvis, S., 2022. Jobos Bay Water Resources II: Using Earth Observations to Analyze Shoreline Changes and Understand the Effects of Sea Level Rise in Southern Puerto Rico (Other - 2022 Spring DEVELOP Technical Paper 20220006785. NASA, p. 17. https://ntrs.nasa.gov/citations/20220006785.
Olofsson, P., Foody, G.M., Herold, M., Stehman, S.V., Woodcock, C.E., Wulder, M.A., 2014. Good practices for estimating area and assessing accuracy of land change. Rem. Sens. Environ. 148, 42–57. https://doi.org/10.1016/j.rse.2014.02.015.
Otero, V., Van De Kerchove, R., Satyanarayana, B., Mohd-Lokman, H., Lucas, R., Dahdouh-Guebas, F., 2019. An analysis of the early regeneration of mangrove forests using landsat time series in the matang mangrove forest reserve, peninsular Malaysia. Rem. Sens. 11 (7). https://doi.org/10.3390/rs11070774. Article 7.

Otero, V., Lucas, R., Van De Kerchove, R., Satyanarayana, B., Mohd-Lokman, H., Dahdouh-Guebas, F., 2020. Spatial analysis of early mangrove regeneration in the Matang Mangrove Forest Reserve, Peninsular Malaysia, using geomatics. For. Ecol. Manag. 472, 118213. https://doi.org/10.1016/j.foreco.2020.118213.
Pesaresi, M., Politis, P., 2023. GHS-BUILT-C R2023A—GHS Settlement Characteristics, Derived from Sentinel2 Composite (2018) and Other GHS R2023A Data. Joint Research Centre (JRC), European Commission. https://doi.org/10.2905/3C60DDF6-0586-4190-854B-F6AA0EDC2A30.
Petrosian, H., Kar, A.D., Ashrafi, S., Feghhi, J., 2016. Investigating environmental factors for locating mangrove ex-situ conservation zones using GIS spatial techniques and the logistic regression algorithm in mangrove forests in Iran. Pol. J. Environ. Stud. 25 (5), 2097–2106. https://doi.org/10.15244/pjoes/62640.
Pham, T.D., Yoshino, K., 2016. Impacts of mangrove management systems on mangrove changes in the Northern Coast of Vietnam. Tropics 24 (4), 141–151. https://doi.org/10.3759/tropics.24.141.
Phong, N.T., Nuong, C.T., 2023. Thinning, selective harvesting and mangrove protection forests: lessons learned and recommendations from the Vietnamese Mekong Delta. Estuar. Coast Shelf Sci. 288, 108345. https://doi.org/10.1016/j.ecss.2023.108345.
Pir Bavaghar, M., 2015. Deforestation modelling using logistic regression and GIS. J. For. Sci. 61 (5), 193–199. https://doi.org/10.17221/78/2014-JFS.
Rakib, M.F., Al-Ansari, E.M.A.S., Husrevoglu, S., Yigiterhan, O., AlMaslamani, I.A., Aboobacker, V.M., Vethamony, P., 2021. Observed variability in physical and biogeochemical parameters in the central Arabian Gulf. Oceanologia 63, 227–237.
R Core Team, 2022. R: A Language and Environment for Statistical Computing, 4.2.2. R Foundation for Statistical Computing. [Computer software]. https://www.R-project.org/.
Raihan, A., Ali, T., Mortula, M., Gawai, R., 2023. Spatiotemporal analysis of the impacts of climate change on UAE mangroves. J. Sustain. Dev. Energy Water Environ. Sys. 11 (3), 1–19.
Red Saudi Global (RSG), 2022. Sustainability report. https://issuu.com/theredsea/docs/rsg_sustainability_report_2022.
Rondon, M., Ewane, B.E., Abdullah, M., Watt, M., Blanton, A., Abulibdeh, A., Burt, J.A., Rogers, K., Ali, P.D.T.A., Reef, R., Mohtar, R., Sidik, F., Fahrenberg, M., de-Miguel, S., Galgamuwa, P., Charabi, Y.A.R., Arachchige, P.S.P., Velasquez-Camacho, L.F., Al-Awadhi, T., et al., 2023. Remote sensing-based assessment of mangrove ecosystems in the Gulf Cooperation Council countries: a systematic review. Front. Mar. Sci. 10, 1241928. https://doi.org/10.3389/fmars.2023.1241928.
Sahadevan, A.S., Joseph, C., Gopinath, G., Ramakrishnan, R., Gupta, P., 2021. Monitoring the rapid changes in mangrove vegetation of coastal urban environment using polynomial trend analysis of temporal satellite data. Reg. Stud. Marine Sci. 46, 101871. https://doi.org/10.1016/j.rsma.2021.101871.
Sanders, C.J., Maher, D.T., Tait, D.R., Williams, D., Holloway, C., Sippo, J.Z., Santos, I.R., 2016. Are global mangrove carbon stocks driven by rainfall? J. Geophys. Res.: Biogeosciences 121 (10), 2600–2609.
Sale, P.F., Feary, D., Burt, J.A., Bauman, A., Cavalcante, G., Drouillard, K., Kjerfve, B., Marquis, E., Trick, C., Usseglio, P., van Lavieren, H., 2011. The growing need for sustainable ecological management of marine communities of the Persian Gulf. Ambio 40 (1), 4–17. https://doi.org/10.1007/s13280-010-0092-6.
Santini, N.S., Reef, R., Lockington, D.A., Lovelock, C.E., 2015. The use of fresh and saline water sources by the mangrove Avicennia marina. Hydrobiologia 745, 59–68.
Saudi Aramco Sustainability Report 2022 https://www.aramco.com/en/sustainability/sustainability-reporteport-Aramco.
Shaltout, K.H., Ahmed, M.T., Alrumman, S.A., Ahmed, D.A., Eid, E.M., 2020. Evaluation of the carbon sequestration capacity of arid mangroves along nutrient availability and salinity gradients along the Red Sea coastline of Saudi Arabia. Oceanologia 62 (1), 56–69.
Sillanpää, M., Vantellingen, J., Friess, D.A., 2017. Vegetation regeneration in a sustainably harvested mangrove forest in West Papua, Indonesia. For. Ecol. Manag. 390, 137–146. https://doi.org/10.1016/j.foreco.2017.01.022.
Silva Junior, C.H.L., Heinrich, V.H.A., Freire, A.T.G., Broggio, I.S., Rosan, T.M., Doblas, J., Anderson, L.O., Rousseau, G.X., Shimabukuro, Y.E., Silva, C.A., House, J.I., Aragão, L.E.O.C., 2020. Benchmark maps of 33 years of secondary forest age for Brazil. Sci. Data 7 (1). https://doi.org/10.1038/s41597-020-00600-4. Article 1.
Simard, M., Fatoyinbo, L., Smetanka, C., Rivera-Monroy, V.H., Castañeda-Moya, E., Thomas, N., Van der Stocken, T., 2019. Mangrove canopy height globally related to precipitation, temperature and cyclone frequency. Nat. Geosci. 12 (1), 40–45. https://doi.org/10.1038/s41561-018-0279-1.
Souza-Filho, P.W.M., Goncalves, F.D., Rodrigues, S.W.P., Costa, F.R., Miranda, F.P., 2009. Multi-sensor data fusion for geomorphological and environmental sensitivity index mapping in the Amazonian mangrove coast, Brazil. J. Coast Res. 1592–1596.
Steppe, K., Vandegehuchte, M.W., Van de Wal, B.A., Hoste, P., Guyot, A., Lovelock, C.E., Lockington, D.A., 2018. Direct uptake of canopy rainwater causes turgor-driven growth spurts in the mangrove Avicennia marina. Tree Physiol. 38 (7), 979–991.
UNEP, 2018. Mangrove Restoration Paying Dividends in Oman. November 1. UNEP. http://www.unep.org/news-and-stories/story/mangrove-restoration-paying-dividends-oman.
Utami, S., Anggoro, S., Soeprobowati, T.R., 2017. The diversity and regeneration of mangrove on Panjang island Jepara Central Java. Int. J. Conserv. Sci. 8 (2), 289–294.
Vaughan, G.O., Al-Mansoori, N., Burt, J., 2019. In: Sheppard, C. (Ed.), The Arabian Gulf. second ed. (Vol. 2, World Seas: An Environmental Evaluation, pp. 1–23. https://doi.org/10.1016/B978-0-08-100853-9.00001-4Elsevier Science.
Van Tricht, K., Degerickx, J., Gilliams, S., Zanaga, D., Battude, M., Grosu, A., et al., 2023. WorldCereal: a dynamic open-source system for global-scale, seasonal, and reproducible crop and irrigation mapping. Earth Syst. Sci. Data Discuss. 2023, 1–36.
Wan, Z., Hook, S., Hulley, G., 2021. MODIS/Terra Land Surface Temperature/Emissivity Daily L3 Global 1km SIN Grid V061. NASA EOSDIS Land Processes Distributed Active Archive Center. https://doi.org/10.5067/MODIS/MOD11A1.061. 2023-12-14 [Data set].
WorldPop, 2020. Population counts 2000–2020 UN-adjusted unconstrained 100m [cited 2024 May 07]. Available from: https://hub.worldpop.org/doi/10.5258/SOTON/WP00660.
Xia, Q., Qin, C.Z., Li, H., Huang, C., Su, F.Z., 2018. Mapping mangrove forests based on multi-tidal high-resolution satellite imagery. Rem. Sens. 10 (9), 1343.
Xia, Q., Qin, C.Z., Li, H., Huang, C., Su, F.Z., Jia, M.M., 2020. Evaluation of submerged mangrove recognition index using multi-tidal remote sensing data. Ecol. Indicat. 113, 106196.
Yancho, J.M.M., Jones, T.G., Gandhi, S.R., Ferster, C., Lin, A., Glass, L., 2020. The Google Earth engine mangrove mapping methodology (GEEMMM). Rem. Sens. 12 (22). https://doi.org/10.3390/rs12223758. Article 22.